Pure Appl. Geophys. 172 (2015), 3357–3384

DOI 10.1007/s00024-015-1128-4

Pure and Applied Geophysics

CrossMark

OSL Dating and GPR Mapping of Palaeotsunami Inundation: A 4000-Year History of Indian Ocean Tsunamis as recorded in Sri Lanka

Ranjith Premasiri,[1,3] Peter Styles,[1] Victor Shrira,[1] Nigel Cassidy,[1] and Jean-Luc Schwenninger[2]

Abstract—To evaluate and mitigate tsunami hazard, as long as possible records of inundations and dates of past events are needed. Coastal sediments deposited by tsunamis (tsunamites) can potentially provide this information. However, of the three key elements needed for reconstruction of palaeotsunamis (identification of sediments, dating and finding the inundation distance) the latter remains the most difficult. The existing methods for estimating the extent of a palaeotsunami inundation rely on extensive excavation, which is not always possible. Here, by analysing tsunamites from Sri Lanka identified using sedimentological and paleontological characteristics, we show that their internal dielectric properties differ significantly from surrounding sediments. The significant difference in the value of dielectric constant of the otherwise almost indistinguishable sediments is due to higher water content of tsunamites. The contrasts were found to be sharp and not to erode over thousands of years; they cause sizeable electromagnetic wave reflections from tsunamite sediments, which permit the use of ground-penetrating radar (GPR) to trace their extent and morphology. In this study of the 2004 Boxing Day Indian Ocean tsunami, we use GPR in two locations in Sri Lanka to trace four identified major palaeotsunami deposits for at least 400 m inland (investigation inland was constrained by inaccessible security zones). The subsurface extent of tsunamites (not available without extensive excavation) provides a good proxy for inundation. The deposits were dated using the established method of optically stimulated luminescence (OSL). This dating, partly corroborated by available historical records and independent studies, contributes to the global picture of tsunami hazard in the Indian Ocean. The proposed method of combined GPR/OSL-based reconstruction of palaeotsunami deposits enables estimates of inundation, recurrence and, therefore, tsunami hazard for any sandy coast with identifiable tsunamite deposits. The method could be also used for anchoring and synchronizing chronologies of ancient civilisations adjacent to the ocean shores.

Key words: Tsunami hazard, Reconstruction of palaeotsunami deposits, Tsunami sediments, Ground-penetrating radar (GPR), Optically Stimulated Luminescence (OSL), Tsunami in the Indian Ocean.

[1] Institute for the Environment, Physical Sciences and Applied Mathematics (EPSAM), Keele University, Keele ST5 5BG, UK. E-mail: p.styles@keele.ac.uk
[2] School of Archaeology, University of Oxford, South Parks Road, Oxford OX1 3PS, UK.
[3] Department of Earth Resources Engineering, University of Moratuwa, Moratuwa, Sri Lanka.

1. Introduction

One of the most promising approaches to evaluate tsunami hazard is through reconstruction of inundations and dates of past events. Coastal sediments deposited by tsunamis (tsunamites) can potentially provide this information, and, therefore, attract intense current interest (Jankaew *et al.* 2008; Monecke *et al.* 2008; Morton *et al.* 2008; Ruiz *et al.* 2008; Yan and Tang 2008). Finding the evidence of inundation remains the most challenging element of palaeotsunami reconstruction. The difficulty is aggravated by the inevitable long-shore variability of tsunamis which has a significant random component (Choi *et al.* 2012). In view of this variability even if the values of inundations or wave height were somehow accurately found in one or two locations this would provide only a relatively weak constraint on tsunami parameters (run-up, number of waves, etc.). Hence, the mapping of inundation or wave height is needed for better constrained estimates. Since the extensive excavation, which is often required, is rarely if ever possible, the use of non-invasive methods is needed. These might include electrical imaging methods and shallow seismic and acoustic methods but these do not have the resolution required (Styles 2011). The non-invasive technique based upon ground-penetrating radars (GPR) utilizes reflections of emitted microwave electromagnetic pulses from subsurface non-uniformities in dielectric properties. The first GPR investigation of a tsunami deposit (washover sand) was carried out by Switzer *et al.* (2006) on the Australian coast, they identified erosional downcutting at the base of the deposit but they did not trace palaeotsunamites as reported here. Very recently GPR has been applied for defining sediment/rock interfaces and the presence of debris with boulders brought in by palaeotsunamis (Koster *et al.* 2013, 2014), i.e. GPR has been used and found effective in situations with a priori large dielectric contrasts between the tsunami deposit and the surrounding topsoil and sand. The big open question is whether the GPR-based approach can work in the generic situations of sandy beaches where tsunamis bring in sand and deposit it upon a sandy beach and there are no noticeable contrasts between the primary physical properties of tsunamite and non-tsunamite sands.

Here, by analysing tsunamites from Sri Lanka identified using sedimentological and paleontological characteristics and confirming and extending our preliminary reports (Styles *et al.* 2007; Premasiri 2012), we show that their dielectric properties differ significantly from surrounding sediments even when the differences in the primary physical characteristics are very subtle. These contrasts cause sizeable electromagnetic wave reflections from tsunamite sediments, which permit the use of ground-penetrating radar (GPR) to trace their cross-shore extent long-shore variations and three-dimensional morphology. In this pilot study we use GPR in two locations to trace four identified major palaeotsunami deposits upon sandy beaches for at least 400 m inland (constrained by inaccessible military security zones). The subsurface extent of tsunamites (not available without extensive excavation) provides a good proxy for inundation (Goto *et al.* 2011; Abe *et al.* 2012). The deposits were dated using the established method of optically stimulated luminescence (OSL), (Huntley and Clague 1996). This dating, partly corroborated by other authors (Ranasinghage 2010, Jackson *et al.* 2014) and available historical records, contributes to a new picture of tsunami hazard in the Indian Ocean.

Quantifying tsunami hazard requires extensive records of magnitudes and dates of past events. Historical records are often insufficient or absent altogether, while for the pre-historical time period, the only available sources are sediments deposited by palaeotsunamis. The first key problem is to confidently differentiate tsunami deposits (tsunamites) from storm surge sediments (tempestites). Micropalaeontological and sedimentological analyses allow such a differentiation as described later (Bryant and Nott 2001; Witter *et al.* 2001; Morton *et al.* 2007; Pratt and Bordonaro 2007; Dahanayake and Kulasena 2008a, b). Dating of the identified deposits can be carried out using several techniques (carbon dating, stratigraphy, thermoluminescence and in appropriate circumstances, tephrochronology) with varying accuracies. If deposits contain quartz sands (very often true, although in Japan these are volcanically derived) OSL is the most appropriate technique (Duller 2008, Bluszcz 2006), enabling dating of events from zero to 150,000 years with accuracies of about 5–10 %. The most difficult and yet unresolved part of the reconstruction is finding the amplitude or/and inundation of the tsunami waves. Several studies have sought clues from the hydrodynamics of tsunamis in geological records with success in determining the number of incoming waves using sedimentological textural analysis (Smith *et al.* 2004; Peters *et al.* 2007; Weiss 2008). However, estimating flow rate or tsunami run-up elevation has proved much more difficult (Morton *et al.* 2007; Peters *et al.* 2007; Bondevik *et al.* 1997; Hindson and Andrade 1999; Moore 2000; Le Roux and Vargas 2005, 2007; Fujino *et al.* 2006; Korycansky and Lynett 2007; ; Moore *et al.* 2007). Recent attempts to link flow velocity and wave heights to grain size distributions are based on a sound fluid mechanical footing (Jaffe *et al.* 2003; Jaffe and Gelfenbaum 2007, Soulsby *et al.* 2007), but permit only rough estimates. Since even solutions of the direct problem have large errors, good quantitative results for the inverse problem are unlikely.

Here, we report work carried out during the PhD thesis of Premasiri (2012) on the potential of palaeotsunami reconstruction based on the previously undiscovered sharp dielectric constant contrasts between tsunamites and normal beach sediments. The contrasts between the dielectric constant of Sri Lankan tsunami deposits and surrounding sediments of other origin measured in the laboratory with very subtle differences in the primary physical characteristics were found to be always large enough for confidently employing GPR for 'direct' probing of morphology of palaeotsunami deposits. Subsequent use of OSL provided dating of the palaeotsunami deposits. The paper reports the testing of this approach carried out on Sri Lanka.

The paper is organized as follows. In Sect. 2, we briefly describe the specific locations on the Sri Lanka coast where we identified palaeotsunami deposits. Detailed studies have been confined to two sites: Hambantota and Yala. In Sect. 3, we describe four different independent approaches (standard grain size statistical analysis, micro-petrography, micro-fossil and mineralogical analyses) we employed for identifying the palaeotsunami deposits in the sedimentological sequence using the 2004-tsunami sediments as a reference. In Sect. 4, we describe our laboratory study of dielectric properties of the sampled sediment showing that the values of tsunamite dielectric constant differ significantly from those of surrounding sediments. The resulting contrasts at the boundaries of tsunami sediment layers which, crucially, were found to remain sharp over thousands of years cause sizeable reflections of electromagnetic waves, which enables us to apply GPR to trace the palaeotsunami deposits. Whereas the previous works simply identified the base of tsunami deposits we show that internal multi-layered structure can be derived using GPR. The successful three-dimensional mapping of the palaeotsunami deposits with GPR in two locations is described in Sect. 5. Section 6 describes the procedure and results of the OSL dating of the collected samples of identified palaeotsunami deposits. Three palaeotsunami events have been OSL dated in the interval between the present day and 3.5 thousand years ago. An additional deeper fourth layer identified as a palaeotsunami deposit could not be OSL dated as the samples were accidentally exposed to light; its date was estimated at ~4000BP by extrapolating the estimated average rate of non-tsunamite deposition. OSL is preferable to radiocarbon dating for these tsunami sediments, as it does not require any knowledge concerning the provenance of organic material.

In Sect. 7, we discuss the available historical evidence and folklore on palaeotsunamis and put our finding into the regional historical perspective. Concluding in Sect. 8, we discuss the potential of this efficient, non-destructive high-resolution technique for tracing palaeotsunami deposits and mapping inundation. The specific implications for Indian Ocean hazard are also discussed.

2. *Locations of the Study and Sedimentological Descriptions*

The research was carried out in an area of the Sri Lankan coast where the 26 December 2004 (Boxing Day) tsunami caused severe impact. Sri Lanka is one of the islands where catastrophic damage was caused even though it is located over 1000 km away from the origin of the 2004 Sumatra Tsunami (Fig. 1). About 75 % of the coast, nearly 1000 km, was affected. The present study mainly concentrates on the south-eastern, southern and western parts of the Sri Lankan coast but detailed analysis is confined to two coastal sites in the southeast of Sri Lanka at the sites shown in Fig. 2 where Quaternary beach deposits (mainly fine-grained garnet-rich, quartz and feldspar mineral sands) overlie Proterozoic metamorphic bedrock, mostly quartz and feldspar-rich granitoid gneisses.

To study coastal stratigraphic sequences and provide ground truth for interpretation of GPR data we dug trenches approximately 1.5 m deep by hand. The 2004 tsunamites are mainly sands, mud, silts and gravel, with occasional organic materials and plant debris and are up to 30 cm in thickness.

The extracted sediment sequences comprise well-stratified beach and fluvial sands, peaty and lagoonal sand or soil interlayered with tsunami deposits. These

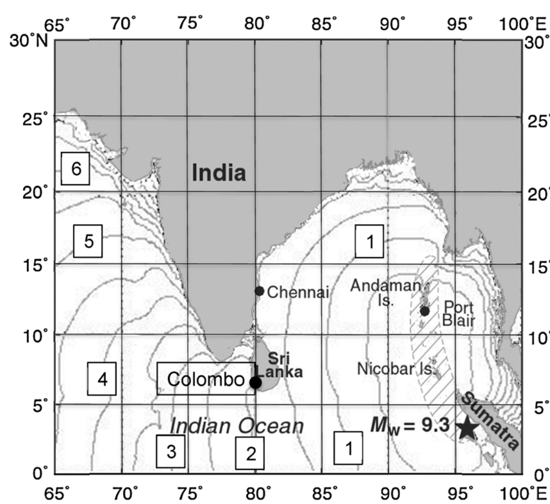

Figure 1

Map of the 2004 Sumatra earthquake epicentre and the surrounding countries affected by the associated tsunami. Isochrones of tsunami travel time at 30 min contours with hourly labels (Fine *et al.* 2005) are also shown together with the inferred rupture zone

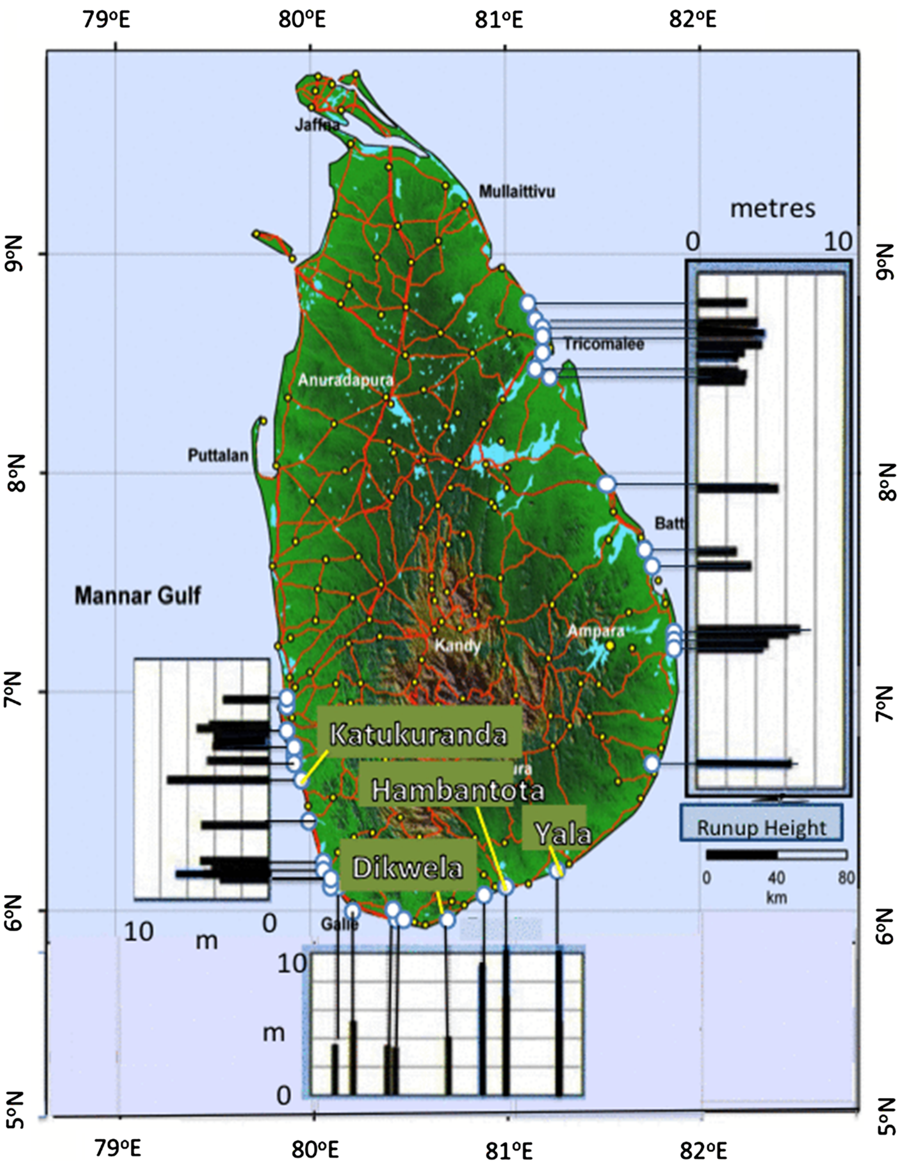

Figure 2

Location map of tsunami sediment studies; Location 1 (Hambantota) and Location 2 (Yala). Dikwela and Katukurunda where GPR profiles were obtained are also shown. *Black bars* the run-up (in metres) observed around the coast of Sri Lanka (pers. comm. Professor A Gunathilake, based on Sri Lanka Geological Survey data, 2005 unpublished information)

different beds are characterized by differing textures, sorting, colour, mineral composition and the presence of shells and fossils. Certain horizons within the sequence are characterized by light colour, poor sorting and comprise gravels or pebbles with fossils and were tentatively inferred to be older palaeotsunami deposits, which has been later confirmed by laboratory analysis on the basis of mineralogical, paleontological, optical microscopic properties. These are discussed fully in Sect. 3.

We used the 2004 tsunamites as a stratigraphic marker, and reference. Both Yala and Hambantota are located on the east–southeast of the island and are likely to have experienced the same general direction of approach (as most great seismic events are located to the east–northeast of the Island) for palaeotsunami deposits as the 2004 Boxing Day tsunami and, therefore, similar pattern of tsunami deposits for the 2004 and palaeo events. In 2004, both sites suffered major inundations of between 500 and 1100 m giving access to sufficiently long profiles to test tracing of the morphology of the deposits using ground-penetrating radar. Figure 2 also shows the run-up and direction of approach based on the study of Hettiarachchi and Samarawickrama (2005) and the run-up observed around the coast of Sri Lanka based on unpublished data from the Sri Lanka Geological Survey (pers. comm. Professor A. Gunathilake).

3. *Sedimentological Analysis and Identification Of 2004 Tsunami Sediments and Palaeotsunami Sediments in Sri Lanka*

Descriptions of sediment package morphology and sedimentary grain size analysis for the 2004 tsunami in Sri Lanka are described in Styles *et al.* (2007) and Dahanayake and Kulasena (2008a, b). The main features of these deposits can be summarized as follows:

- Sand deposits of varying thickness (massive sandy deposits in some places) from a few centimetres to over 30 cm thick) were observed all around the island
- Sediment deposition was higher on the southeast and eastern coasts than on the western coast. The tsunami deposits in Sri Lanka are mainly confined to low relief topographical features such as swells or marshlands. Sediment deposition patterns were more often controlled by local topographical features than by the tsunami wave characteristics.
- The extent of deposition of tsunami sediment inland is strongly dependent on the inundation distance. Both were measured independently. Sediment deposition was observed over at a maximum of 700 m inland at these localities (although much greater distances were observed elsewhere around Sri Lanka) as continuous beds, discontinuous sheets, lenses, and pocket-like deposits.
- Layered deposits were often observed with the number of sediment depositional packages, observed at any location corresponding to the number of waves.
- The tsunamite sediment deposits on the coastal zone from the tsunami were easily distinguishable from normal beach sediments because of their contact morphology (erosive and with the lower contact downcutting peaty or normal dark coloured top soils) and their textural characteristics (often coarse-grained, poorly sorted and light coloured).
- Isolated large boulder deposits (which are called tsunami-ishi by Kato and Kimura 1983) reflect the high-energy hydrodynamic regimes, and the sandy deposits contain rip-up clasts showing a very energetic environment during the deposition and in fact some regions of the coastline were sometimes subject to erosion rather than deposition.

Following and extending Styles *et al.* (2007) and Premasiri (2012) we identify the features listed below as distinctive characteristics of the 2004 tsunami sediments on the Sri Lankan coast.

1. Tsunami sediment depositional characteristics are strongly dependent on local topographical variation and the nature of back-wash flow. The sediment mainly consists of poorly sorted, medium-to-coarse sand.
2. While tsunami sands are not identical to normal beach sand in composition, texture structure and most other physical characteristics they often show compositional heterogeneity and it is difficult to identify them on sedimentological characteristics alone and such identifications should be treated cautiously.
3. The first 50 to 75 m distance from the coast is mainly subjected to erosion rather than deposition.
4. No strong relationship exists between sediment thickness and wave characteristics such as wave direction or run-up height.
5. Mineralogically, tsunamite sands are rich in quartz and feldspar minerals with other heavy or opaque minerals and Fe/Mg silicate minerals present in significant amounts as compared to normal beach sand (Herath 1985, 1988).
6. The tsunami sands from Sri Lanka show mechanical fracturing at microscopic scales. The specific mechanism of fracturing is not identified; this goes beyond the scopes of the present study. The observed fracturing may be an indicator of provenance rather than process.

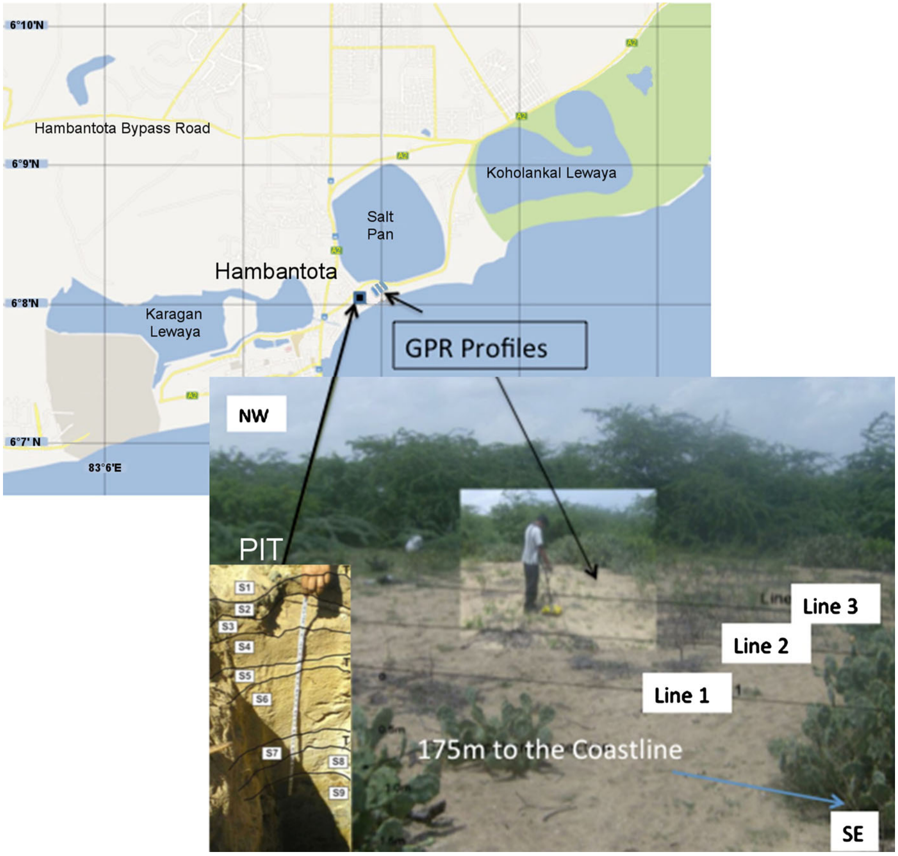

Figure 3
Location of the pit dug for palaeotsunami studies at Location 1 (Hambantota 6.13°N, 81.13°E). The location of the excavated pit and the GPR *Survey lines* are shown

7. With time, the uppermost layer of the tsunami sediments can be altered by natural environmental causes; these changes may depend on sediment type, climatic conditions and height of deposition (Spiske *et al.* 2013). However, the effect decreases inland and the impact on thicker deposits is less pronounced. We resampled tsunami sediments after a period of 3 years and found no discernible difference.

3.1. Grain Size Statistical Analysis

3.1.1 Location 1: Hambantota, Southeast Coast of Sri Lanka

Location 1 is a flat beach ridge adjacent to Hambantota-Mahalewaya lagoon where sediment deposition displayed thicknesses exceeding 30 cm for the 2004 tsunami. In July 2008, a 1.5-m-deep trench, located about 175 m inland at an elevation of 0.3 m was dug by hand (Fig. 3), until it reached the lagoon clay bed. Samples were taken for paleontological and sedimentological analysis and OSL dating This area was severely affected by the 2004 tsunami and an associated sediment layer a few centimetres thick could be observed. The stratigraphic section (Fig. 4a) displays conspicuous layering in the sandy sediments. The 2004 tsunami sediment (S1) was clearly identified lying on top of the original peaty ground.

It was also possible to identify a further two layers (S5 and S7) comprising light-coloured, coarse-grained sediments with properties distinct from the background sediments which are inferred from field observation to be palaeotsunami sediments. Grain size analyses and statistical analysis were performed for each tsunami sediment sample collected from

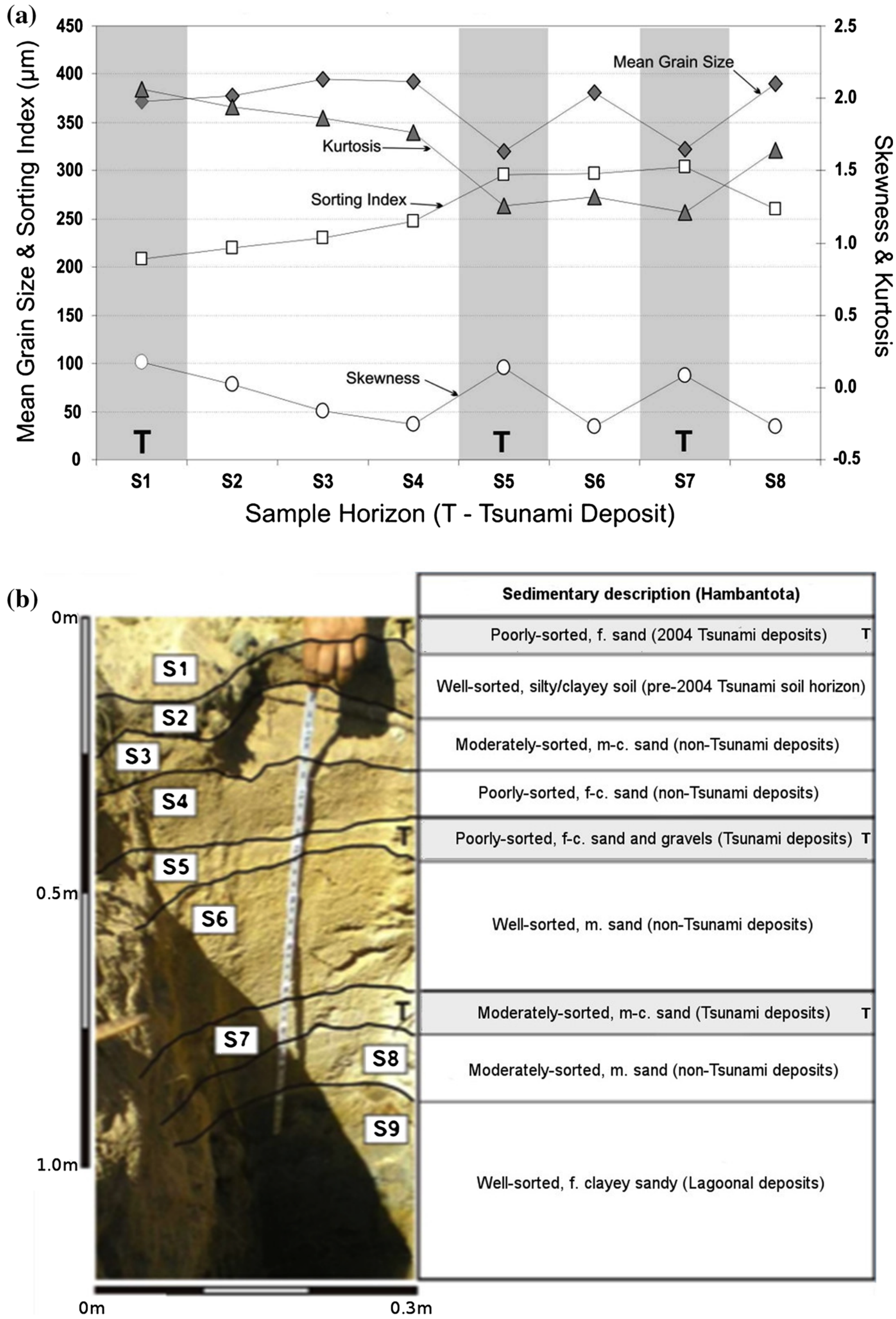

Figure 4

a Palaeotsunami sand layers and non-tsunami deposits (beach sand, fluvial sands and lagoonal clayey sand) at Location 1, Hambantota (layers are labelled as S1, S2 up to S9). Notation: *f* fine, *f–c* fine-to-coarse, *m* medium, *m–c* medium-to-coarse, *T* tsunami sediments. **b** Statistical characteristics of grain size distribution at Hambantota

both the 2004 tsunami and presumed palaeotsunami deposits (distinguished because of their distinctive colour and texture from the lagoonal sediments) as follows. 400–500 g samples were collected from each layer and sub-sampled by the cone and quartering method and then 100 g of sediment were used for the

Table 1

Sedimentological parameters for the Hambantota and Yala tsunami (italicized numbers) and non-tsunami deposits

Site	Sample	Tsunami Deposits				Fluvial, Marine, Lagoon Deposits			
		Mean Grain Size	Kurtosis	Skewness	Sorting Index	Mean Grain Size	Kurtosis	Skewness	Sorting Index
Site 2—Yala	S1	*377.9*	*2.05*	*0.44*	*190.3*				
	S2					349.9	2.25	0.32	201.2
	S3/4	*214.6*	*2.46*	*0.93*	*242.3*				
	S5					451.5	2.24	−0.56	222.4
	S6	*282.5*	*4.42*	*1.12*	*142.4*				
	S7					320.5	4.10	0.92	141.3
	S9					358.9	2.55	0.19	181.2
	S10	*346.5*	*2.86*	*0.71*	*165.6*				
Site 1—Hambantota	S1	*371.7*	*2.06*	*0.18*	*208.6*				
	S2					377.2	1.94	0.02	219.9
	S3					394.6	1.86	−0.16	230.0
	S4					393.0	1.77	−0.26	247.4
	S5	*320.0*	*1.26*	*0.13*	*295.8*				
	S6					380.9	1.32	−0.27	296.9
	S7	*322.4*	*1.21*	*0.08*	*304.0*				
	S8					390.4	1.64	−0.27	259.7
	SD	56.6	1.10	0.41	62.3	36.2	0.81	0.44	45.2
	Median	322.4	2.06	0.44	208.6	380.9	1.94	−0.16	222.4
	Mean	319.4	2.33	0.51	221.3	379.7	2.19	−0.01	222.2

sieve analysis. The samples were fractionated into grain size using standard sieve sizes, described by Syvitski (1991). Some sites had extremely fine-grained layers; the 2004 tsunami sediment deposit at Katukurunda underwent grain size analysis using a Malvern Mastersizer X Ver. 1.2b. Statistical parameters of the grain size distributions such as mean grain size, standard deviation (sorting index), skewness (deviation from a symmetrical Gaussian curve either in a positive or negative direction, i.e. towards coarser or finer grains), and kurtosis (a measure of 'peakiness' where the distribution is more/less sharply peaked than a standard Gaussian bell curve) were determined using the Gradisat software (Blott and Pye 2001) calculated on the basis of the percentile statistics of Folk and Ward (1957).

To provide the context we mention that sorting values may be used to determine the wave period. Sediment layers with higher sorting values may suggest that the sediment has been created by a shorter wave period (Wagner and Srisutam 2011). High values of skewness (positively skewed) correspond to a grain size distribution with a modal peak corresponding to medium-grained sands with the tail corresponding to coarser grained sediments. Low skewness values (negatively skewed) correspond to grain size distributions in which there is a significantly finer tail element. Low kurtosis values usually correspond to grain size distributions which are narrower than Gaussian unimodal distributions. High kurtosis values correspond to broader and flatter, often poly-modal, grain size distributions (Dawson *et al.* 1996a, Wagner and Chanchai 2011). In the adopted normalization the Gaussian distribution has kurtosis equal to one.

From the grain size statistical analyses (Table 1; Fig. 4b), we observe that layers S5 and S7 (inferred palaeotsunami) as well as the 2004 tsunami sediment S1 exhibit small positive skewness, while all other layers have negative skewness. However, these differences in the grain size distributions we consider to be too subtle to serve for robust identification of the tsunami sediments.

Table 1 and Fig. 5 both show that tsunami and non-tsunamite deposits are strongly bi-modal in grain size with no immediately obvious differences between them; it would be difficult to make a firm identification simply on sedimentological grounds alone without associated field observation as discussed by (Engel and Brückner 2011).

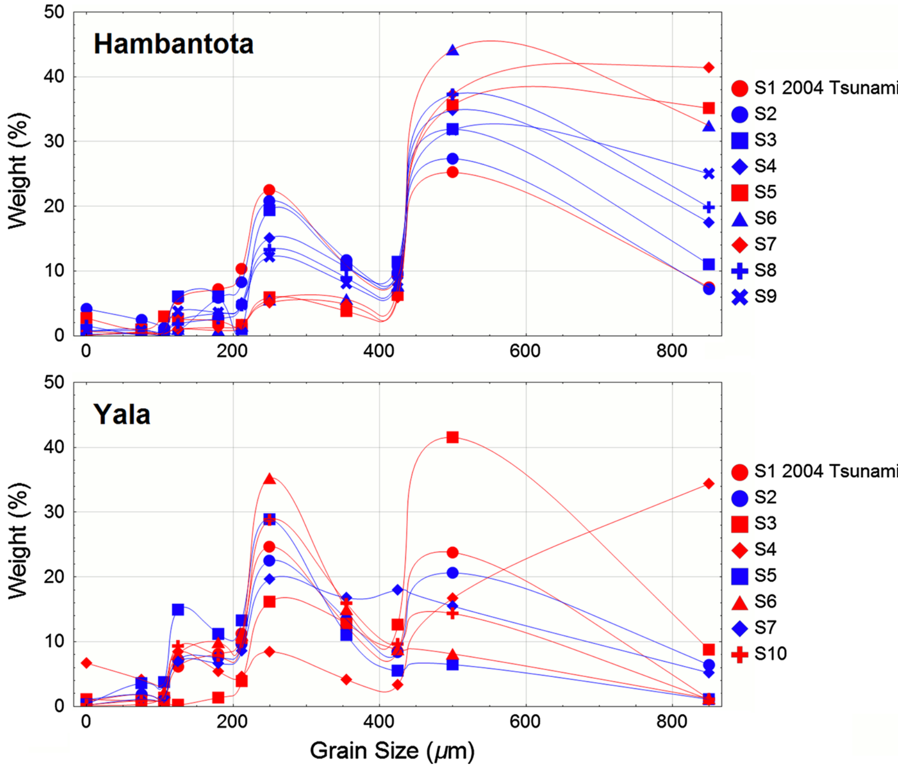

Figure 5
Grain size distributions of tsunami and palaeotsunami (*red*) and beach sediments (*blue*) at Location 1 (Hambantota) and Location 2 (Yala) (color figure online)

3.1.2 Yala, Southeast Coast of Sri Lanka

Location two was on flat ground at the boundary of the Yala National Wild Life Park. The location was severely affected by the 2004 tsunami, which caused massive damage. In July 2008, a 1.5-m-deep trench, located about 250 m inland at an elevation of 0.3 m above mean level was dug by hand until it reached the lagoon clay bed (Fig. 6). Samples were taken for paleontological and sedimentological laboratory analysis and OSL dating.

The sediment sequence at the location shows well-marked sediment layers (Fig. 7) with distinctly different textural/structural properties and colour. The topmost layer of the sequence (S1) is the 2004 tsunami sand deposit, which is recognized from its erosive lower contact with the original peaty ground surface.

Three other light-coloured, coarse-grained sediment layers (S3/4, S6 and S10) have been identified as tsunamite (palaeotsunami) sediments and are clearly visually distinguishable from other coastal beach sediments on the profile, although the definitive identification is possible only in the laboratory. The grain size distribution patterns of tsunamite sediment do not differ greatly from other sediments, showing similar poly-modal distributions and increased coarse fraction. Although these tsunamite sediment layers show positive skewness, which is not typical of the non-tsunami sediment, these signatures although consistent are considered to be too weak to be a basis for robust distinguishing of tsunami deposits.

3.2. Micro-petrographic Studies

Petrographic studies were carried out on sediment samples from the two locations Hambantota and Yala, using plane-polarized and cross-polarized illumination. A few samples from Hambantota are shown at two different magnifications in Fig. 8a–e. The tsunamite sediments from layers S1 and S5 are

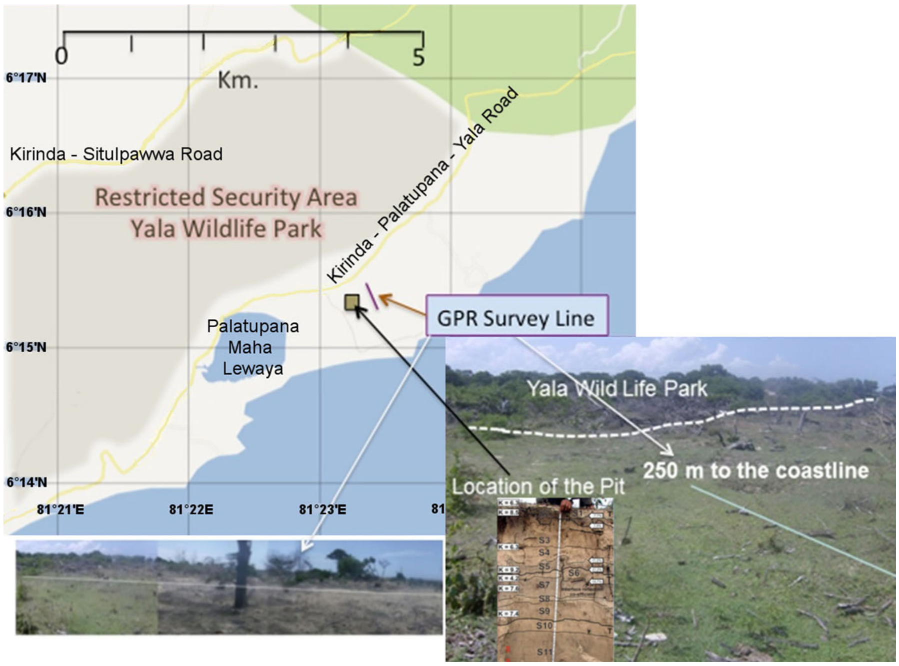

Figure 6
Map of the palaeotsunami studies carried out at Location 2 (Yala 6.25°N, 81.39°E). The position of the excavated pit and the GPR Survey Line are shown

poorly sorted comprising a wide range of grain sizes from fine to very coarse. They mainly comprise well-rounded to angular grains of quartz and feldspars with trace amounts of opaque and Fe–Mg Silicate minerals. Most of the quartz and feldspar grains exhibit micro-fracturing (Fig. 8a, e). The precise mechanism of this fracture process is yet to be established, here we speculate that it is the much more energetic processes involved in tsunami entrainment and deposition as compared to normal beach processes; the issue goes beyond the scope of the present work.

Non-tsunami sediment layers of S2, S3 and S4 from Hambantota comprise mainly fine-to-medium-sized grains, that are moderately to well sorted, angular to sub-rounded. Their mineral composition was mainly quartz and feldspar with a characteristic feature being that they are more opaque and with a larger component of Fe–Mg silicate minerals than are seen in the tsunamite sediments of S1 and S5.

3.2.1 Petrographic Studies at Hambantota

Petrographic studies were also carried out using plane-polarized and cross-polarized illumination. Some samples are shown at two different magnifications in Fig. 9a–e. Left-hand pictures in 9a, 9b and 9d are at 6.3× magnification while the right-hand pictures are at 2.5× magnification, under cross-polarized light. Figure 9c shows the fossil assemblages present.

3.2.2 Petrographic Studies at Yala

Samples were also collected at Yala. The Yala tsunamite sediments show similar micro-petrographic characteristics to those of location 1 (the Hambantota site). They exhibit poor sorting from fine-to-coarse sand, the presence of micro-fracturing, large quartz and feldspar grains, angular to well-rounded mixtures of grains and very low Fe–Mg silicate and opaque mineral content (Fig. 9a, c). The sections of layers S5 and S7, which are identified as non-tsunamite sediments show relatively smaller grain size and better sorting together with a higher composition of Fe–Mg opaque minerals (Fig. 9b, d).

The normal beach sediments contain higher compositions of Fe–Mg minerals (Fig. 9b, d) because they are principally of continental

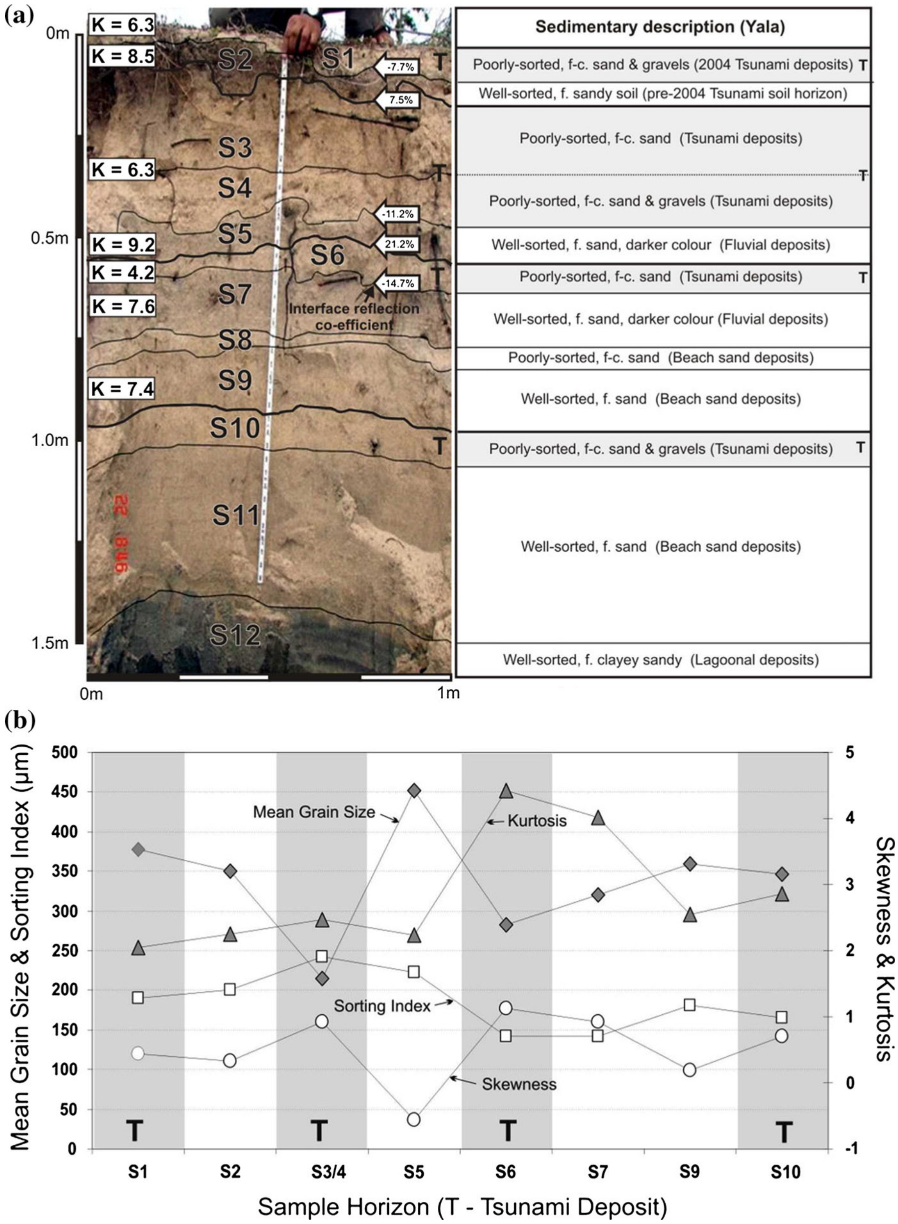

Figure 7

a Tsunami sand layers and non-tsunami deposits (beach sand, fluvial sands overlying the lagoonal clayey sand) at Location 2, Yala (layers are labelled as S1, S2 up to S12). Notation: *f* fine, *f–c* fine to coarse, *m* medium, *m–c* medium-to-coarse, *T* tsunami sediments, *K* electromagnetic impedance contrast. **b** Statistical characteristics of grain size distribution at Yala

provenance and derived locally; the tsunami by contrast mobilizes much more distal sediment which is impoverished in Fe–Mg minerals. This is an additional specific robust discriminating feature between Sri Lankan tsunamite sediments and normal beach deposits.

3.3. *Micro-fossil Analysis of Palaeotsunami Sediments*

Microfossils from both 2004 tsunami and older palaeotsunami sediments have been identified and studied in detail (Dahanayake and Kulasena 2008b; Premasiri 2012). The 2004 tsunami sediment samples

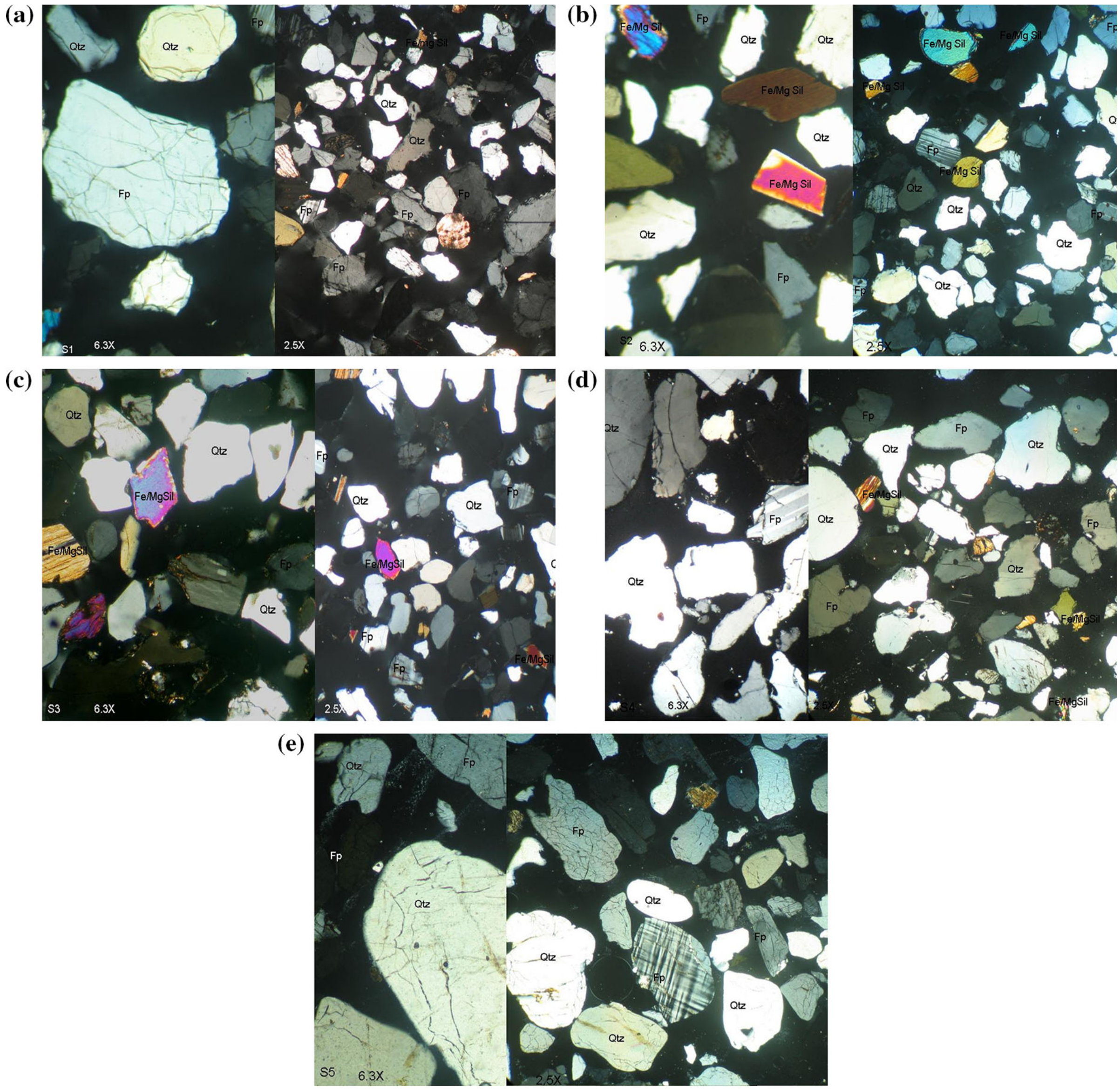

Figure 8

Micro-petrographic images of different sediment layers of coastal sediment sequences at Hambantota (Location 1). *Left-hand side panels* are at ×6.3 magnification and *right-hand side panels* are at ×2.5 magnification, under polarized light. *FeMgSi* Feldspar, *Qtz* Quartz. **a** Layer S1: 2004 Tsunami sediments. Note the strong fracturing present in the quartz grains. **b** Layer S2: non-tsunami sediments (Soil Horizon). The micro-fracturing is not displayed here. Quartz grains can be clearly seen in the *left-hand panel*. **c** Layer S3: non-tsunami; beach sediments. **d** Layer S4: non-tsunami sediment; fluvial. **e** Layer S5: palaeotsunami sediments. Note very strong fracture fabric in the quartz grains on the *left*

were studied at many locations (Fig. 11): Katukurunda (Kaluthara), west coast, Karaganlewaya (Hambantota), southeast coast, Palatupana (Yala), southeast coast and microfossils were analysed for palaeotsunami sediments from Hambantota (Pit at Location1) and Yala (Pit at location 2). One of the most distinctive features of the palaeotsunami sediment deposits we have studied on the Sri Lankan coast which is shared by the 2004 tsunami sediments is the presence of different species of microfossils in all the tsunamite layers (identified on the basis of totality of the features) and their absence in all other

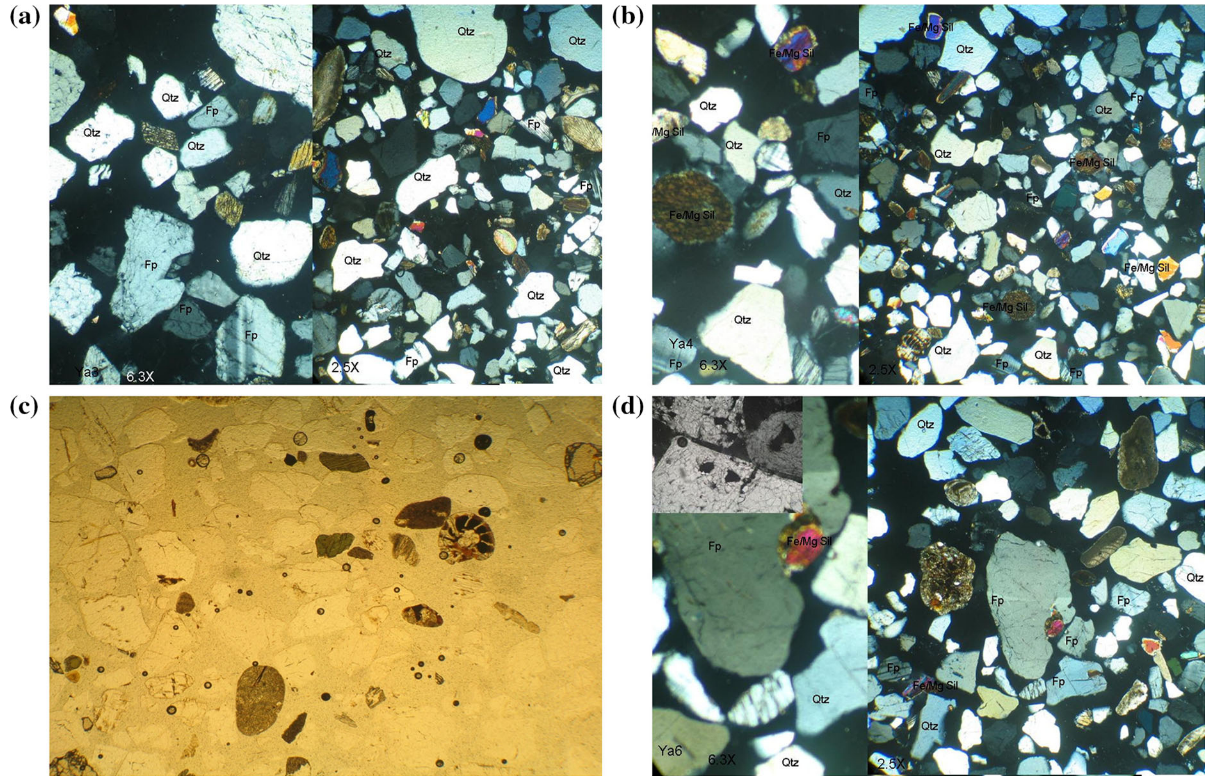

Figure 9
Micro-petrographic images of different sediment layers of coastal sediment sequences at Yala (Location 2). *Left-hand side pictures* are at ×6.3 magnification and *right-hand side pictures* are at ×2.5 magnification, under polarized light. *FeMgSi* Feldspar, *Qtz* Quartz. **a** Layer S3: palaeotsunami sediments, no fractured Quartz. **b** Layer S5: non-tsunamigenic sediments, no fractured Quartz. **c** Layer S6: palaeotsunami sediments showing fossil assemblages in plane-polarized light. A number of foraminiferal species are present (Premasiri 2012). **d** Layer S7: non-tsunamigenic sediment, no fractured quartz

layers. Most of the microfossils have been identified as extinct benthic and large benthic species of (Dawson *et al.* 1996b) which belong to a wide age range. Taxa identified after both reflection microscopy and scanning electron microscope (SEM) studies by (Dahanayake and Kulasena 2008a, b) and by (Premasiri 2012) are described in detail in (Premasiri 2012).

3.4. Identification of Palaeotsunami Sediments

Although the palaeotsunami sediments are characterized by positive skewness and exhibit strong negative correlations between grain size and skewness ($r = -0.8$ to -0.9) and a less pronounced relationship between mean grain size and kurtosis ($r = -0.6$ to -0.9) (Table 1) we do not employ these features for discriminating tsunamites, relying instead upon more robust methods of identification.

Micropalaeontological analysis of the 2004 and palaeotsunami deposits shows that, in contrast to sediment layers of other origin, they contain diverse foraminifera. Since three different, totally independent tsunami diagnostic criteria (micro-petrography, microfossil and mineralogical analyses) are satisfied for five distinct layers in the sedimentological sequence with the 2004 Boxing Day sediments serving as a reference, we identify the lower four of them as palaeotsunamites.

4. Laboratory Analysis of the Dielectric Properties of Tsunami Sediments

Ground-penetrating radar uses electromagnetic waves in the frequency range from c 50 MHz up to

1 GHz, emitted from specialized tuned antennae placed directly on the ground surface. The electromagnetic waves of this range are modified by propagation through geological materials, being attenuated strongly by conductive layers including significant clay content and saline water but propagating well through quartz-rich sediments such as beach sands (Figs. 4, 7). GPR-based techniques have been used extensively for mapping the internal configuration of sandy deposits such as dunes (Jol 2008). Where there are sharp changes in electromagnetic (dielectric) properties (electrical resistivity and magnetic susceptibility) strong reflections take place with the reflected waves received on complementary tuned antenna enabling these interfaces to be traced for large distances (Ezzy *et al.* 2003, 2011). The signals attenuate with depth due to energy loss and absorption but in favourable circumstances penetrations of some tens of metres and reflections from multiple layers and their geometries and spatial relationships can be clearly seen. The use of shallow GPR for other sedimentological purposes has been widely reported (e.g. Meyers *et al.* 1996; Tamura *et al.* 2008) and its use for environmental applications is described in detail in Styles *et al.* (2011). GPR is an established, non-invasive, high-resolution geophysical technique with wide application for imaging shallow sedimentary sequences for sedimentological and stratigraphic studies and has been successfully utilized for mapping several differing types of Quaternary quartz-rich clastic deposits but only recently (Koster *et al.* 2013, 2014) in the tsunami context. Our laboratory measurements of samples taken from our sites show that tsunamite dielectric properties differ significantly from ambient soil and normal beach sediments, causing distinct reflections from the boundaries of the tsunamite layers, with reflection coefficients shown in Table 2 for the site at Yala. The dielectric properties of saturated sediments from the Yala site show that very high reflection coefficients of between 7 and 21 % exist at interfaces between the tsunami-deposited sedimentary layers and the beach/lagoonal layers. Measurements were also made on a subset of dry samples where the reflection coefficients are all about 1 %. On this basis we suggest that the water content residing within the complex internal pore geometry of the immature, poorly sorted sediment of the tsunami deposits plays a critical role in the differential increase of the dielectric constant of tsunamites, which results in the generation of the observed continuous and very distinct reflections from the tsunami deposit boundaries. Pinpointing the specific properties of tsunamite sand grains which lead to a higher porosity of the tsunamites and hence result in such strong contrasts in water content and dielectric properties remains an outstanding fundamental problem outside the scope of this work. Here, we just note that since normal beach sand grains are more rounded than the sand grains deposited by tsunami, we can hypothesize that more rounded grains allow tighter packing and hence less voids providing space for water.

This dielectric study work was carried out at Keele University, and not all sediment samples were available for analysis but the dielectric properties (relative permittivity) of the identified tsunami and non-tsunami sediments from the sediment profile at Yala, Sri Lanka (S1, S3/4, and S6 are tsunami

Table 2

Dielectric properties of saturated sediments from the Yala site

Sample (Yala site)	S1	S2	S3/S4	S5	S6	S7	S9
Dielectric constant K	6.27	8.53	6.32	9.92	4.19	7.58	7.43
K lower error limit	5.23	7.30	5.03	8.71	3.72	6.17	6.78
K upper error limit	7.32	9.77	7.61	11.13	4.66	8.99	8.07
Loss tangent	0.11	0.11	0.11	0.09	0.11	0.12	0.13
Attenuation (dB/m)	15.46	20.11	15.89	18.45	12.41	18.76	21.64
Velocity (m/ns)	0.120	0.103	0.119	0.095	0.146	0.109	0.110
Reflection coefficient at basal interface (%)	−7.7	7.5	−11.2	21.2	−14.7		

Measurements were also made on a subset of dry sample and the reflection coefficients are all less than 0.011 showing that the water content within the internal geometry of the samples is critical sediment layers) for both 'dry' and 'wet' conditions have been measured using the standard method following the procedure described in Jol and Bristow (2003). In situ, the sediments are almost always wet and so the samples were rewetted with distilled water thus restoring their ambient saturation levels ($\sim$25 % by volume moisture content). The samples were then packed into the measurement cell to equal density/volume ratios and the relative permittivity (dielectric constant, K) measured at the central GPR frequency of 500 MHz. Results from these wet sediments are shown in Table 2. The frequency dependence of dielectric properties of sand in this range is known to be small (Mätzler and Murk 2010) and so these measurements are also representative for the GPR antennae employing frequencies in the range 450–900 MHz.

We are primarily interested in the reflection coefficients (R) at a sedimentary layer boundary

$$R = (\sqrt{K2} - \sqrt{K1})/(\sqrt{K2} + \sqrt{K1}),$$

where $K1$ and $K2$ are the dielectric constants in the adjacent layers. The coefficients characterize the normalized amplitudes of reflections between the adjacent layers in the sequence. The table demonstrates a noticeable change in dielectric constant between the tsunamites and the adjacent non-tsunamite layers, which, therefore, leads to strong negative reflection coefficients at the bases of the tsunami layers. The subtle differences in the primary physical characteristics of sediment grains (prevalence of angular shaped grains, grain size, sorting, etc.) affect the microscopic volumetric moisture content variation across the interfaces that, in turn, lead to significant macroscopically averaged dielectric property contrasts.

Where sedimentary layer interfaces are sharp, laterally coherent and have metre-scale planar geometries, observable GPR reflections can be obtained from relatively low values of reflection coefficient (<3 %) and here we have reflection coefficients, which far exceed this. Such characteristics are common in both aeolian and fluvial sedimentary environments where GPR-based studies have been highly successful (Bristow 2009).

The distinct dielectric signatures of the tsunamite sediments provide the rationale for the use of ground-penetrating radar in the field. Indeed, at the two locations described above the existence of strong reflected signals from each tsunami sediment layer has been confirmed and allowed us to discriminate the very clear layered pattern of tsunamite sediments even in cases exhibiting only subtle differences in the primary physical characteristics.

5. *Subsurface Mapping of Palaeotsunami Sediments Using the GPR Technique*

To reconstruct the 3D distribution of the tsunamite deposits a non-invasive remote sensing technique is needed. Since our trench excavations indicated shallow, thin layering and thanks to our discovery of a dielectric constant anomaly for the tsunamites, GPR is an ideal technique for tracing the subsurface configuration of the tsunami deposits on the Sri Lankan coast. In this study, two pilot GPR surveys aimed primarily at testing the feasibility of the approach were carried out at two previously described sites (Fig. 2), Yala, Hambantota. GPR traverses normal to the coast at 2.5–5 cm intervals were collected with a PulseEkko PE1000 system using 450 and 900 MHz antennae, and processed with standard methods (Jol and Bristow 2003).

More specifically, the GPR profiles were acquired with a Pulse Ekko GPR system with 450 MHz antennae as a sum of short (12.43 m) segments with spacing between acquisition points of 25 cm and with bistatic, parallel antenna geometry with an antenna spacing of 20 cm. The data were sampled at 0.1 ns giving 632 time samples per trace.

The data were processed using the Open Source MATGPR processing package in Matlab: (http://users.uoa.gr/~atzanis/matgpr/matgpr.html) and the processing sequence is described in detail in "Appendix".

Figures 10, 11, 12, and 13, show the raw (unprocessed) and processed GPR data. The detailed interpretation has been overlain on the Yala profile (Fig. 10) but the interpretation of the others is shown in Figs. 14 and 15.

While some features can be seen in the shallowest portions of the raw data they are obscured by pulse shape as the signal has not been adjusted to remove

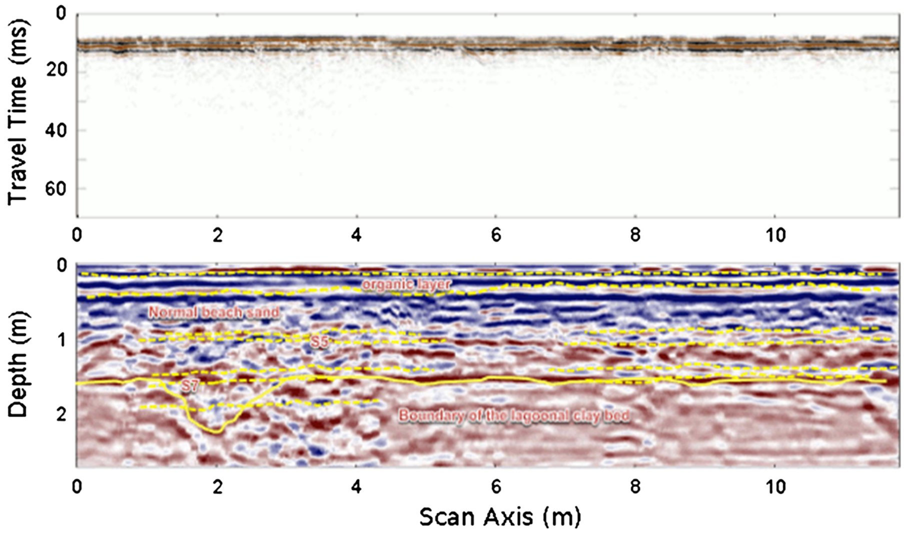

Figure 10
Yala. A 19m segment of the GPR survey line shown on Fig.6. *Upper panel* raw GPR data. *Lower panel* reprocessed and depth converted data. The interpretation of this profile has been overlaid. Coastline is to the *left*

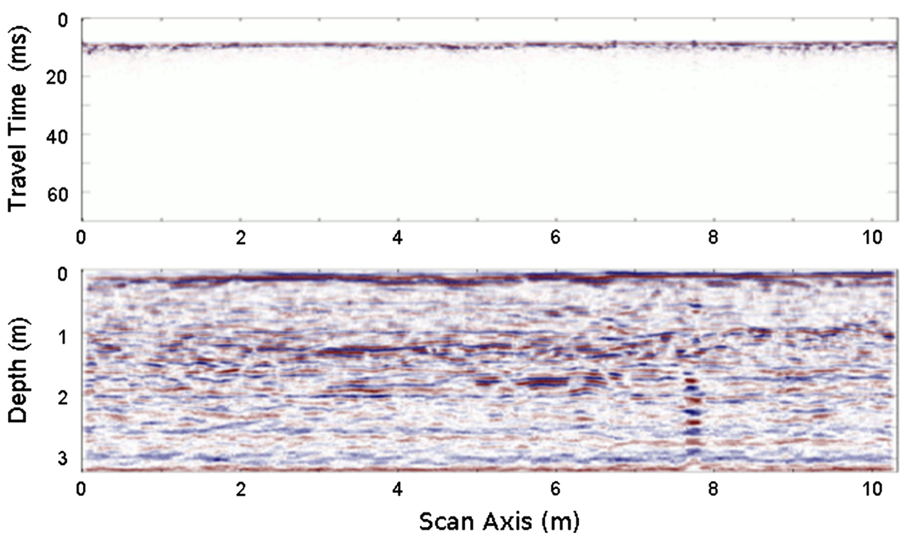

Figure 11
Line 1 Hambantota. *Upper panel* raw GPR data. *Lower panel* reprocessed and depth converted data. Coastline is to the *right*

this by deconvolutions or for geometric spreading ("Appendix") and, therefore, we cannot resolve the deeper layers until after processing when we can clearly make out strong continuous reflections extending across the whole section and down to depths of a few metres. Although there is strong reflection from the water table since it is not a perfect reflector some penetration does occur, which enables us to see a layered structure beneath. The improvement in the clarity and interpretability of these processed sections can be clearly seen. Separate bespoke processing of the very shallowest layers may be able to reveal more detail about the depositional characteristics of the 2004 tsunami and further acquisition is planned to explore this. While dune forests were recognized at other sites (Dikwela) they

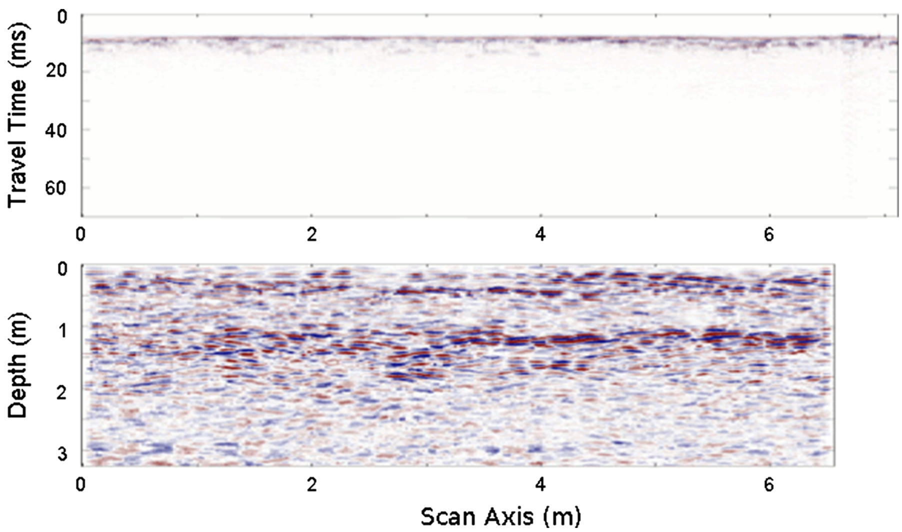

Figure 12
Line 2 Hambantota (as in Fig. 11)

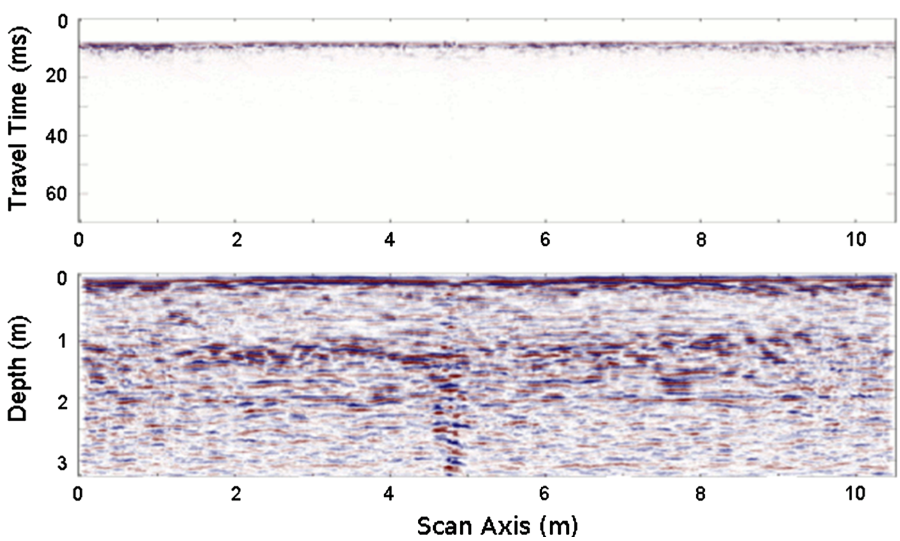

Figure 13
Line 3 Hambantota (as in Fig. 11)

were not present on the GPR profiles here which is indicative of differing flow regimes.

Figure 14 shows an interpretation of the Yala traverse (Fig. 10), where we have identified tsunamite sediment layers based on trenches/pits and geological studies and it was possible to unequivocally trace tsunamite sediment layers with GPR. The validation of the reconstruction was provided by the ground truth data. We also collected samples for OSL dating from these sites. From the GPR survey at Hambantota, two tsunami layers could be traced from all three GPR sections, while at Yala three sediment layers from palaeotsunami events could be traced up to 250 m inland (Fig. 16). The surveys could not be continued further inland because of the security restrictions due to civil war at the time of the field study. Two additional GPR surveys were carried out at Dikwela and Katukuranda (see map on Fig. 2), where there were no indications for tsunamite sediment from trenches or geological field studies to

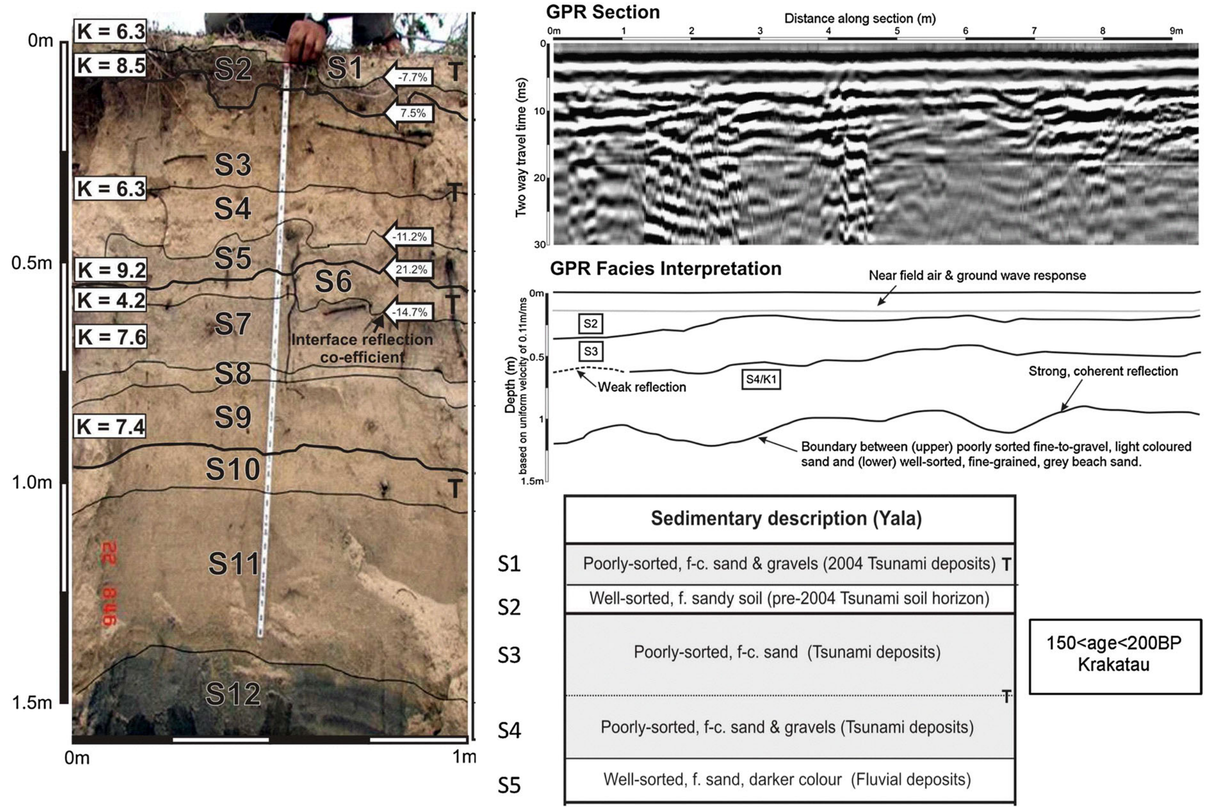

Figure 14

Field identification of palaeotsunamites and correlation with the GPR profile and its interpretation at Yala. *K* is the electromagnetic impedance which is the contrast between layer boundaries; it determines the reflection coefficient and the layering observed on the GPR section

correlate with the GPR sections. GPR profiles from these sites do not show any positive indications of palaeotsunamite sediments as were recognized at sites Yala and Hambantota (Premasiri 2012). The GPR section at Dikwella gave no indication of the presence of coarse-grained sand deposits interlayered with the marshy clay beds and GPR interpretation of site at Katukurunda showed no evidence for the occurrence of palaeotsunami sediment layers in the beach sand profile. They present as normal beach sand deposits exhibiting cross bedding; ripple marks and other poorly differentiated sand layers with textural and mineralogical variations.

These extra GPR surveys (Premasiri 2012) illustrate the point that palaeotsunami sediments are not preserved everywhere in the areas inundated by the 2004 tsunami as sometimes the environment is erosive rather than depositional, and obviously we should expect that tsunami deposits might be present in some areas and not in others. However, where the tsunamite deposits do occur in the coastal deposits they manifest as very distinctive geological layers compared with the normal beach deposits and the GPR technique can be invaluable for mapping them.

The results of the laboratory electromagnetic measurements show a clear contrast between the dielectric properties of the tsunamite sediments and normal beach sands and lagoonal sediments (Table 2), which is the reason for the clearly defined reflection signatures observed on the GPR profiles. Inspection of the reflection coefficients shows that for all of the tsunami deposits examined here there is a strong negative reflection coefficient, which defines the tsunami event. The lower values of dielectric constant in the tsunami deposits are consistent with a decrease in pore space and, therefore, water content associated with the less rounded sand grains observed in these sediments.

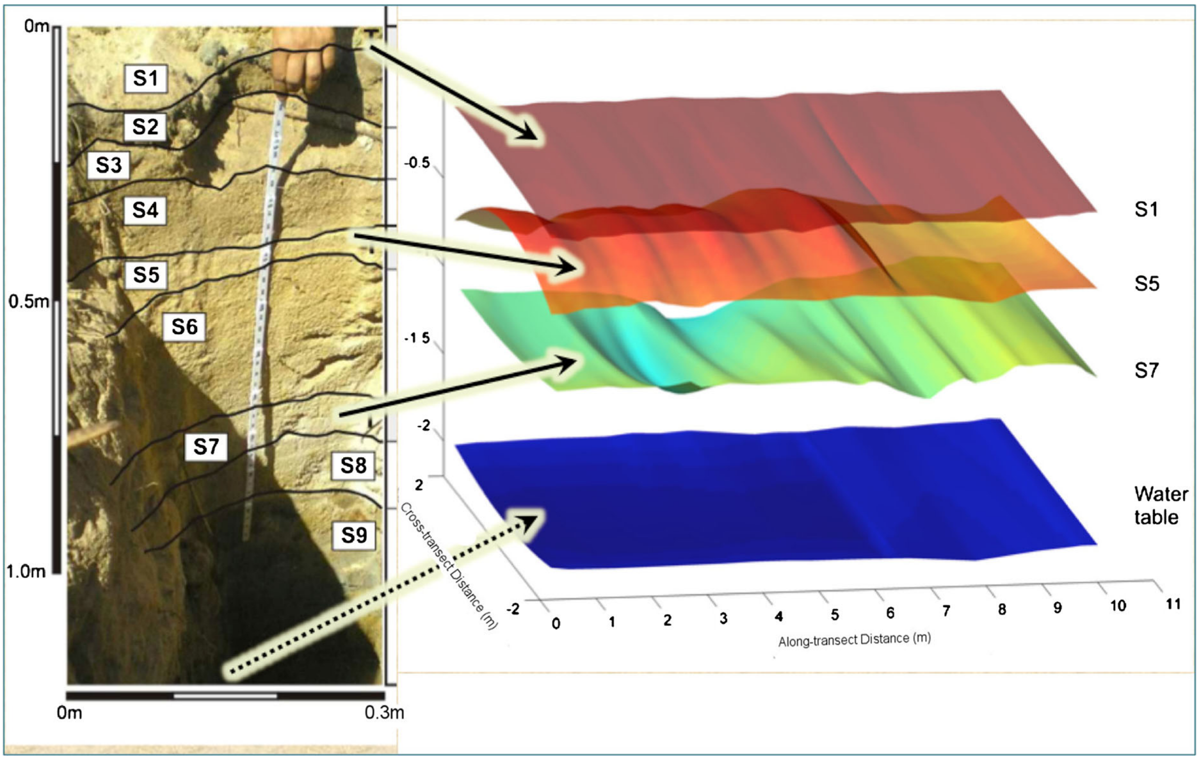

Figure 15
Three-dimensional view of the lower surfaces corresponding to tsunami and palaeotsunamite layers identified by GPR (S1, S5 and S7) in this study at Hambantota showing that even with these limited data sets the three-dimensional topography of the interfaces can be retrieved. The vertical variations are exaggerated

The dating of the sediments discussed below allows us to conclude that the dielectric contrasts remain sharp over several 1000 years (at the very least!) which allows this technique to be used for Palaeotsunami sediment mapping.

At Hambantota we acquired three parallel closely spaced radar sections (lines 6, 9 and 17 in Figs. 11, 12, 13) and we were able to trace at least three palaeotsunami sediment layers identified visually in the excavated trenches. These were confirmed to be tsunamites by laboratory analysis and were traced from 150 to 400 m from the coastline. Three-dimensional projections of the tsunami depositional surfaces derived from these sections are shown in Fig. 15. Tsunami deposits with varying thicknesses and continuity continue further, but restricted security access at that time (although access may be available in the future) precluded tracing them beyond 400 m from the coast. The 2004, benchmark tsunamites are visually observed to extend at least 600 m inland at this location (Hambantota). We are able to produce the internal configuration of the palaeotsunami depositional surfaces. Thus, we identify four major palaeotsunami deposits, all almost certainly associated with major geological catastrophes. Similar results were obtained at the Yala location (Fig. 2), but could not be traced as far inland due to marshland and security restrictions.

Geological and sedimentological studies reveal that tsunamite deposits are confined to certain specific locations on the coastal zone and they have varying thicknesses within continuous or discontinuous sheets or layered deposits. These deposits are preserved within coastal sediment sequences or in low-lying marshy clay beds. The dielectric constants of these sediments were found to differ sufficiently from the surrounding normal beach and lagoonal sediments to provide significantly large electromagnetic reflections at the layer boundaries to enable them to be traced using GPR. The cross-shore extent

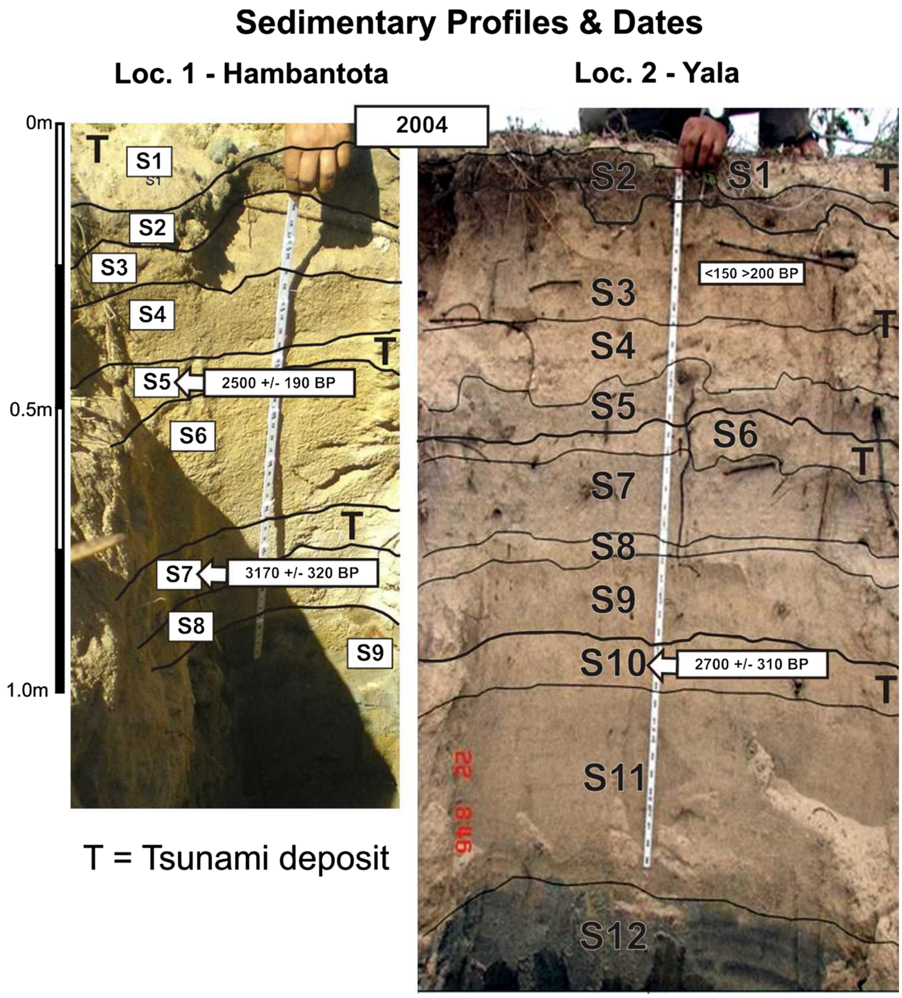

Figure 16
Optically stimulated luminescence dating of palaeotsunami sediment layers at Hambantota and Yala

of the tsunamite deposit supported by mapping of its lateral dependence is a key input parameter for determining the tsunami amplitude which deposited these palaeotsunamites. Recent successful applications of GPR for mapping Quaternary deposits and several types of coastal sand deposits are described in (Botha *et al.* 2003; Havholm *et al.* 2003; Heinz and Aigner 2003; Jol and Bristow (2003); Woodward *et al.* 2003). However, Koster *et al.* (2013, 2014) and now this work is the first applications of GPR for mapping tsunamite deposits and this is certainly the first application to Sri Lanka which is not itself tsunamigenic and so experiences only mega-tsunamis generated at great distances.

6. OSL Dating of Palaeotsunami Sediments on the Sri Lankan Coast

Luminescence dating is based on the time-dependent dosimetric properties of silicate minerals, predominately feldspar and quartz (Bos and Wallinga 2009). The technique has been used to date sediments, usually <200,000 years old, that received sunlight exposure prior to deposition (Hashimoto *et al.* 1986). Exposing sediment to sunlight for hours or heating to above 300 °C eliminates most of the previously acquired luminescence from mineral grains. After the sediment is buried and shielded from further light exposure ionizing radiation from the decay of naturally occurring radioisotopes of U, Th, and K produces free electrons which are subsequently trapped in crystallographic charge defects in silicate minerals. Excitation of minerals by heat or light causes recombination of stored charge, which results in luminescence emissions. The intensity of the luminescence is calibrated in the laboratory to yield an equivalent dose [De, measured in grays (Gy); 100 rads = 1 gray], which is divided by an estimate of the radioactivity that the sample received during burial (dose rate, Dr) to give a luminescence age (Wallinga 2002). When sediment is buried, the effects of the incoming solar radiation are removed. With this bleaching effect removed, a signal accumulates within individual mineral grains (most commonly quartz and feldspars). It is this signal that is the key to luminescence dating techniques. Given an estimate of the rate of received ionizing radiation and knowing the total accumulated dose (the palaeodose) it is possible to derive an age since burial (Murray and Wintle 2000).

Samples were collected from Yala and Hambantota where the detailed GPR studies were carried out, from each layer identified as a tsunami deposit. To collect samples for OSL dating without exposing them to sunlight, opaque polyvinyl tubes (12 cm length and 5 cm diameter) were used as sample containers and the sample was collected directly into the tube while inserting the tube horizontally into the geological profile and both ends of the tube were shielded immediately. The samples were analysed at the Oxford University Luminescence Dating Laboratory using single-aliquot procedures (Murray and Wintle 2000). Three identified palaeotsunami events have been OSL dated at 150 to 200 BP, 2550 ± 190 BP, 2710 ± 310 BP (probably the same event within the error bounds) and 3170 ± 320 BP years by combining the data from the two profiles (Fig. 16).

In addition to these three OSL-dated palaeotsunami sediments layers, we did identify a fourth layer as a palaeotsunami but samples from the oldest fourth layer were accidentally exposed to light and could not be OSL dated; we plan to resample this layer. Meanwhile, we crudely estimate its date at ~4000 BP by extrapolating the estimated average rate of non-tsunami sedimentation; since three older tsunami deposits with ages of 4200, 4500, and 5000 B.P. have been found on the same stretch of the coast in Kirinda (6.2277°N, 81.3349°E) and Okanda (6.6554°N, 81.7695°E) Lagoons (Ranasinghage 2010) this is a credible postulate.

7. *Palaeotsunami Records from the Indian Ocean and Region and Their Record on the Sri Lankan Coast*

In this study, we confidently identify and can trace for some considerable distance palaeotsunamites with ages: 150–200 BP, 2550 ± 190 BP, 2710 ± 310 BP (probably the same event within the error bounds) and 3170 ± 320 BP. Previous studies (based on carbon dating) on the coast of Thailand and Sumatra have shown a recurrence interval of mega-tsunamis in the Indian Ocean of nearly 600 years. They report four palaeotsunami events at 100–130 BP, 540–600 BP, 966–1170 BP, 2200 BP and at 3050 BP (Bondevik 2008; Jankaew *et al.* 2008; Monecke *et al.* 2008; Brill *et al.* 2011, 2012). The first palaeotsunami event in this sequence is the 1883 Krakatau eruption tsunami. This tsunami as well as the 2004 Sumatra one originate from the Sumatra region, which is considered to be the most significant potential tsunami-generating source in the Indian Ocean. (Table 3).

Three older tsunami deposits with ages of 4200, 4500, and 5000 B.P. have been found in Kirinda (midway between Hambantota and Yala) and Okanda Lagoons (inland from Yala, 6.6554°N, 81.7695°E), (Ranasinghage 2010) and Abeyratne *et al.* (2007) dated with radiocarbon a sand layer at 4829 ± 362 B.P. in Kirinda Lagoon. A further deposit from Panama Lagoon (6°45′–6°46′N, 81°48–81°49′E) has a reported age of 6817 ± 132 B.P. (Ranasinghage 2010).

In a very recent paper, Jackson *et al.* (2014) report the results of coring in the coastal lagoons from Karagan Lagoon in south-eastern Sri Lanka that provide evidence for palaeotsunami deposits at 2417 ± 152 B.P. to 2925 ± 98 B.P., which we report here. Premasiri (2012), traced the same deposits with GPR for a significant distance although as we have no OSL dates we do not discuss it further here. Jackson *et al.* (2014) also identified six older tsunamis

Table 3

Palaeotsunami records for the Sri Lankan coast and the Indian Ocean from the present study and the literature

Event	Date	References	This study	Historical records and legend
1	2004	Sumatra Tsunami	2004 (Sumatra)	2004 Sumatra Mega Tsunami
2	1883	Newspapers, colonial archives Choi *et al.* (2003), Pelinovsky *et al.* (2005)	150–200 BP	Krakatau eruption
3	100–130 BP	Brill *et al.* (2012)	Not recognized	1881 Rupture of the Sunda Arc
4	380 + 130 BP	Jankaew *et al.* (2008)	Not recognized	
	540–600 BP	Prendergast *et al.* (2012)		
	500–700 BP	Brill *et al.* (2011)		
5	990–1400 BP	Prendergast *et al.* (2012)	Not recognized	
	966–1170 BP	Monecke *et al.* (2008)		
6	2200 BP	Monecke *et al.* (2008)	2500 ± 190 BP	Viharamahadevi Event (Sri Lanka)
	2100 ± 260	Prendergast *et al.* (2012)		
7	3050 BP	Brill *et al.* (2012) identified an event in Phra Thongs as marine sand but it may be a palaeotsunamite)	3170 ± 320 BP	Mentioned in the Ramayana (c3000 BP) Thailand

between 4064 ± 128 B.P. and 6665 ± 110 B.P. They do not seem to have identified the event at 3179 ± 320 BP which we can trace at Hambantota, as we have noted above, not all events are preserved everywhere depending on coastal orientation and littoral topography. This event appears to have historical corroboration as we describe below.

7.1. Krakatau Event

The 1883 tsunami caused by the Krakatau eruption was reported by numerous eyewitnesses and was widely described in newspaper articles of the day (e.g. Sunday Observer of 27th August 1883). However, there are no quantitative data and, in particular, the run-ups were not recorded, eyewitnesses reported heights of c. 1 m (Choi *et al.* 2003). All available information was summarized in (Choi *et al.* 2003, Pelinovsky *et al.* 2005) where the Krakatau tsunami was modelled retrospectively utilizing all the data worldwide. The model yields the maximum wave amplitude at Sri Lanka coast of c.3.6 m, the calculated run-up height at Colombo was 0.5 m.

7.2. Princess Viharamahadevi's Tsunami

There are no contemporary historical records confirming the precise date corresponding to the tsunami event, which deposited the layer S5 for which the OSL dating yields 2500 ± 190 BP. However, the event left a lasting historical impression, which has survived as a legend, first as an oral tradition and then in written form, to the present day. The legend links the event to King Kelanitissa who ruled over a part of Ceylon from the second century BC and his daughter, Princess Viharamahadevi. The king sacrificed Viharamahadevi by sailing her out to sea in a golden vessel to protect the populace from giant sea waves, which inundated most of the coast. This story has been reported in classical historic Sri Lankan chronicles, Mahawamsa and Rajawaliya (Suraweera 2000; Sumangala 1996; Codrington, 1994; Hardy 1866).

We provide long quotes from the books to identify key actors, some of which are known contemporary historical figures and to give an idea of the scale of devastation brought by that tsunami.

> The queen of this king (king of Kelaniya) Tissa had carried on an intrigue with her brother-in-law, who on being detected fled and corresponded with her by a messenger disguised as a priest. The man attached himself to the attendants of the chief priest who was visiting the palace, and catching the eye of the queen dropped his master's letter. Unfortunately the palm-leaf missive made a noise in falling; the correspondence was detected, and the king in his fury slew not only the messenger but also the chief priest, whose complicity he suspected. Thereupon the sea, which according to the Rājāvaliya was then about seven gaus (some fifteen miles) from Kelaniya, overwhelmed the

land, submerging many towns and villages. To put an end to this the king placed his daughter Dēvī in a golden vessel and launched it into the sea: she was carried southwards and cast ashore near the temple (vihāra), when she became the queen consort of Kākavanna Tissa under the name of Vihāra Dēvī. Their sons were Gāmani Abhaya, the future hero, and Tissa.

This quote from (Hardy 1866) identifies the key actors, which at least partially are known historical figures and suggests the inundation distance at 15 miles at Kelaniya, whose location has not been definitely established. The second quote from (Codrington 1994) adds some colourful, but difficult to interpret, details on the scale of devastation:

…to punish the king for this act of impiety towards an innocent priest, the déwas who protect Ceylon caused the sea to encroach on the land, and much damage was done to the country. To appease their wrath, as it was supposed that the country could be saved in no other way, the king resolved to sacrifice his virgin daughter. Placing her in a golden vessel, on which was inscribed the word "rájathítáti", which signified that she was a royal maiden, the vessel was committed to the waves of the sea. But the flood still raged, until 100,000 towns, 970 fisher villages, and 470 villages inhabited by divers for pearls, had been submerged. As the king, from the back of his elephant, was watching the progress of the devastation, the earth opened, and flame burst forth from beneath, and he was no more seen by his people. By this time twenty miles of the coast, extending inland, had been washed away, and the distance from Kalyáni to the sea was reduced to four miles. The royal virgin drifted towards the dominions of the king of Mágam, when some fishermen, who brought it to land, saw the vessel. The monarch Káwantissa, having heard of the wonderful capture made by the fishermen, went to examine it; and when he had read the inscription upon it, he released the princess from her confinement, and she became his queen.

King Dtugamunu, the son of the princess is a prominent historic figure; the period of his reign is considered to be well established. According to Suraweera (2000) and (Sumangala 1996), he ruled during the interval 161-137 BC, which is close to the OSL dating of 2550 ± 190 BP. The accuracy of the OSL dating could be improved by analysing more samples and by calibrating the results using the known date of the 1883 Krakatau event; however, this goes beyond the scope of the present work.

It should also be mentioned that in November 325 BC (c. 2330 BP), the fleet of Alexander the Great was seriously damaged by a tsunami-like event in the mouth of the Indus (Arrian *et al.* 2004). This tsunami was observed about 1500 km to the North-West of Sri Lanka but this date lies within the error bars of our OSL dating of the layer at 2550 ± 190 BP. While this correlation is tentative at best it is interesting to speculate that the two might be related. However, it is also possible that this was more likely to be of local origin rather than basin-scale, as it may have been caused by an earthquake located within the Makran Subduction Zone, which is a region that has produced numerous earthquakes in recent times (e.g. Byrne *et al.* 1992). However, clarification would require significant extra work and identification and dating of tsunamite sediments from sites around the Gulf of Aden, East African and Indian coasts.

7.3. Earlier Events

Layer 7 at Hambantota, which has been identified as a tsunamite, has an OSL age of 3170 ± 320 BP and there is at least a mentioning in historical records of a tsunami which may have been around that time. Wattegama (2005) describes seven significant tsunamis to hit Sri Lanka, the second has already been correlated with the event at c. 2500 BP but he refers to an earlier event, which he calls 'Tsunami One' and is recorded in the epic poem the Ramayana.

The Ramayana is one of the two great Indian epics, the other being the Mahabharata, and describes life in India around 1000 BCE, i.e. 3000 BP. There are many translations/interpretations and their provenance is of variable reliability but all of these share a common belief that there was a great tsunami which devastated the region and so this must have occurred c. 3000 BP.

Sita is projected as the daughter of the Earth. Symbolically, Sita is a small landform or island which emerges out of a big Earthquake or

Volcanic Eruption in the sea. Rama is the symbolic representation of the people from India who invade or conquer the new land form, Sita, with bow and arrows. Lanka is an island and Raven represents the people who settle there. Raven conquers Sita by making the setters run away. Hanuman is the son of the God of Wind or Storm and he is capable of burning Lanka and putting a mountain in the sea so that India and Lanka can be connected. It means out of a Volcanic Eruption, the city of Lanka is burned out and new mountain in the sea emerges connecting India and Lanka. Crossing the sea, through the newly emerged land, Rama conquers Lanka. By a Tsunami, Sita disappears and Rama immerses in the water. Since the sons of Rama and Sita were on the mainland, they escaped. (http://drrajumathew.wordpress.com/2011/03/22/ramayana-the-story-of-a-great-tsunami-in-india-told-symbolically/).

Earlier tsunami events in Sri Lanka seem to have left no traces in collective memory, although at the times of the tsunami which deposited the fourth postulated tsunamite in the sediment sequence at Hambantota which on stratigraphic arguments may possibly be older than 4000 ±/−500 BP, the island had been populated and there was a developed civilisation. There are clear layered sequences on the GPR records which lie beneath those which we have identified and dated in our pits and Jackson *et al.* (2014) have demonstrated that at least 6 further tsunamis lie in this age range. We believe that these can also be identified and traced to determine inundation distance and hence through modelling estimate tsunami run-up height and potentially by comparison between different localities the epicentre and magnitude of the causative seismic event.

Thus, the dates of two of the three recent palaeotsunami events, estimated as between 150 and 200 years BP, 2550 ± 190 and 3170 ± 320 years BP, are corroborated by historical records. The youngest layer clearly corresponds to the recorded 1883 Krakatau event, while the second youngest might correspond either to the major tsunami reported in Sri Lankan chronicles during the reign of King Kawantissa at about 2200BP or a tsunami encountered by Alexander the Great's fleet in 325 BC on the shores of the North Arabian Sea (Wijetunga 2008). Carbon dating studies on the coasts of Thailand and Sumatra (Jankaew *et al.* 2008; Monecke *et al.* 2008) report three events: 1300–1450 AD, 780–900 AD and 2200 BP, suggesting a recurrence interval of circa 600 years for this seismically active part of the Indian Ocean, The Sri Lankan sites, far from any seismically active zones, reflect only the basin-scale events with a correspondingly longer recurrence interval (poorly constrained) at circa 850 years. Our potential circa 4000 BP event appears to be confirmed by the results of Jackson *et al.* (2014).

Reconstruction of palaeotsunami magnitudes based upon estimates of inundation is sensitive to sea-level variations. The only recorded Holocene sea-level rises which are reported as gradual around Sri Lanka of about one metre each are well established from coral studies and radiocarbon dating (Katupotha and Fujiwara 1988; Woodroffe and Horton 2005) at 5500 ± 500 BP and 2750 ± 400 BP. Therefore, interpretation of the two youngest of the three recent palaeotsunami events examined here, the Krakatau and Princess Viharamahadevi tsunamis, can rely upon the level and position of the present coastline. For the two older events one metre correction should be factored in.

8. Conclusions

We have demonstrated that ground-penetrating radar is an efficient non-destructive high-resolution technique for tracing palaeotsunami deposits and mapping inundation on the shores of Sri Lanka. The discovered significant contrasts in dielectric properties between deposits and surrounding soil even with only subtle differences in their primary physical characteristics are expected to be generic and a potential physical mechanism linked to the higher water content has been identified. The recent papers by Koster *et al.* (2013, 2014) from other regions (Spain, Greece, Arabian Sea) have exploited the robustness of the contrasts and applicability of GPR for a variety of geological and geomorphological contexts. The contrasts were found to remain sharp over thousands of years. Complemented by OSL dating, this allows evaluation of local tsunami hazard through an estimation of tsunami inundation and frequency distribution.

The specific implications for Indian Ocean hazard follow from the remoteness of Sri Lanka from seismically active areas; the four palaeotsunami deposits identified here must have left traces on most Indian Ocean shores aiding discrimination between 'local' and 'basin scale' events. Our estimate of the recurrence interval of 'basin-wide' events as circa 850 years is based on dating of just four palaeotsunami deposits with the oldest tentatively dated at c. 4000 BP. It is noticeably larger than the c. 600 years recurrence interval estimated for Sumatra and Thailand (Bondevik 2008; Jankaew *et al.* 2008; Monecke *et al.* 2008; Brill *et al.* 2011, 2012). All the above estimates are weakly constrained and to improve them one needs going to older tsunamites. In our pilot project, GPR clearly shows layered structures well below the c. 4000 BP event; presumably these correspond to the older events identified in cores by Jackson *et al.* (2014). We cannot confirm these, as the dug pits cannot extend as deep as sediment coring. However, radiocarbon dating by Jackson *et al.* (2014) indicates that the recurrence interval may range from as short as 181–517 years to as long as 1045 ± 334 years, in this upper part of the sequence and our value is within this range.

While coring of sediments can clearly give a longer time range than we have currently obtained using GPR, they only give a snapshot at individual localities of the sediment distribution especially for palaeotsunamites and it is not practicable to excavate the whole area. The ability to correlate and trace these tsunamites using GPR permits a robust estimate of the most landward inundation and hence tsunami run-up.

Since the time horizon for OSL dating is much greater than the ages of palaeotsunami we have recorded here, the combination of the pits, coring and GPR suggests that further reliable age estimates could be obtained when security restrictions are lifted. Increasing the number of sampled locations will further improve the accuracy of dating, which could be also used for synchronizing of chronologies of ancient civilisations adjacent to the ocean shores.

Acknowledgments

The authors are grateful to the anonymous referees for the thorough reading of the manuscript and helpful comments.

Appendix: GPR Processing Sequence

The following processing sequence was applied to the Sri Lankan GPR data:

1. Zero adjust (static shift)—during a GPR survey, the first waveform to arrive at the receiver is the air wave., which is delayed due to propagation in the connecting cables. We, therefore, need associate zero-time with zero-depth, so that any time offset due to instrument recording is removed before interpretation of the radar image. This is done individually for each radar section but in this survey was typically about 7 ns.
2. Background removal—background noise is present due to ringing in the antennae, producing a coherent banding effect across the radar section. We sum all the amplitudes of simultaneous reflections along a profile and divide by the number of traces to give a composite signal, which is an average of all background noise which is then subtracted from the data.
3. Gain—gain compensates for amplitude variations in the GPR image as early signal arrival times have greater amplitude than later arrival times because of geometric spreading and intrinsic attenuation. Time-variable gain functions are to equalize the amplitudes of the recorded signals constant along the trace. We have used an inverse amplitude decay gain, which compensates for both geometric spreading and attenuation simultaneously in conjunction with automatic gain control, which balances the signal amplitudes and emphasizes more subtle features.
4. Frequency filtering—GPR data are collected with source and receiver antennae of specified dominant frequency, however, the recorded signals include a band of frequencies wider than this specific frequency. Frequency filtering removes undesirable higher and/or lower frequencies to produce a more interpretable GPR image. This is

called band-pass filtering and in this survey a pass band was selected interactively for each section but typically this covered a range of 0.1–3.0 GHz.

5. Deconvolution—the recorded radar signal is the interaction between the layered earth and its reflecting horizons which depend on electromagnetic contrast (which is what we require) and the radar source function, which is generated by reflection at each interface and adds to the final recorded signal. Deconvolution is the inverse filtering operation that attempts to remove the effects of the source wavelet to better interpret GPR profiles as images of the earth structure. There many different deconvolution methodologies but the one, which we have used, is known as sparse deconvolution (i.e. the Earth has mostly zero reflectivity with a few 'sparse' strong reflectors) with a Blackman–Harris (a sum of weighted shifted sinc functions) window.
6. Median filter—this enhances the continuity of reflector signals by replacing each value by the 5×5 median of the values around it.
7. Depth conversion—the radar sections are converted from time to depth using the velocities determined experimentally in the laboratory and the depth correlation established in the field.
8. Colour scale—finally, an appropriate colour scale and set of brightness values is chosen to produce a good interpretable radar section. This is a subjective process but can make significant improvements in clarity.

References

Abe, T., Goto, K., Sugawara, D. (2012), *Relationship between the maximum extent of tsunamis and the inundation limit of the 2011 Tohoku-oki tsunami on the Sendai Plain, Japan, Sedimentary Geology*, *282*, 142–150.

Abeyratne, M., Jayasingha, P., Hewamanne, R., Mahawatta, P., and Pushparani, M.D.S. (2007), Thermo-luminescence dating of palaeotsunamis and/or large storm-laid sand deposits of small estuary in Kirinda, southern Sri Lanka. A preliminary study. In Proceedings of the 23rd Annual Session, Geological Society of Sri Lanka, p. 6.

Arrian, Anabasis Alexandri: Book VIII (Indica), (Kessinger Publishing Co, ISBN-10: 1419106783; ISBN-13: 978-1419106781, Whitefish, Montana, USA, 2004).

Blott, S.J. and Pye, K. (2001), *Gradisat: A grain size distribution and statistics package for the analysis of unconsolidated sediments, Earth Surface Processes and Landforms*, *26*, 1237–1248.

Bluszcz A., OSL Dating in Archaeology, in Impact of the Environment on Human Migration in Eurasia (Eds. Scott E. M., Alekseev A. Y. and Zaitseva G), (Springer Netherlands 2006) pp. 137–149.

Bondevik, S., Svendsen, J.I., Johnsen, G., Mangerud, J., and Kaland, P.E. (1997), The Storegga tsunami along the Norwegian coast, its age and runup, Boreas, *26*, 29–53.

Bondevik, S. (2008), *Earth science: The sands of tsunami time*, Nature, *455*, 1183–1184.

Bos, A.J.J. and Wallinga, J. (2009), *Analysis of the quartz OSL decay curves by differentiation*, Radiation Measurements *44*, 588–593.

Botha, G.A., Bristow, C.S., Porat, N., Duller, G.A.T., Armitage, S.J.,Roberts, H.M., Clarke, B.M., Kota, M.W., Schoeman, P. Evidence for dune reactivation from GPR profiles on the Maputaland coastal plain, South Africa, In: Ground Penetrating Radar in Sediments, (eds. Bristow, C.S. and Jol, H.M.), (Geological Society, London, Special Publication, 2003), vol. *211*, pp. 29–46.

Brill D., Brückner H., Jankaew K., Kelletat D., Scheffers, A and Scheffers S. (2011), *Potential predecessors of the 2004 Indian Ocean Tsunami Sedimentary evidence of extreme wave events at Ban Bang Sak, SW Thailand*, Sedimentary Geology, *239*, 146–161.

Brill D., Klasen N., Brückner H., Jankaew K., Scheffers, A., Kelletat D. and Scheffers S., (2012), *OSL dating of tsunami deposits from Phra Thong Island, Thailand*, Quaternary Geochronology, *10*, 224–229.

Bristow, C.S., Ground penetrating radar in Aeolian dune sands. In., Ed. Ground Penetrating Radar: theory and applications. (ed. Jol, H.M) (Elsevier Science, 2009) pp. 273–297.

Bryant, E.A. and Nott, J. (2001), *Geological indicators of large tsunami in Australia*, Natural Hazards, *24*, 231–249.

Byrne, D. E., L. R. Sykes, and D. M. Davis (1992), *Great thrust earthquakes and aseismic slip along the plate boundary of the Makran Subduction Zone*, J. Geophys. Res., *97*(B1), 449–478.

Choi, B.H, Pelinovsky, E., Kim, K. O. and Lee, J.C. (2003), *Simulation of the trans-oceanic tsunami propagation due to the 1883 Krakatau volcanic eruption*. Natural Hazards and Earth System Sciences, *3*, 321–332.

Choi, B.H, Min, B. I., Pelinovsky, E., Tsuji, Y. and Kim, K. O. (2012), *Comparable analysis of the distribution functions of runup heights of the 1896, 1933 and 2011 Japanese Tsunamis in the Sanriku area* Nat. Hazards Earth Syst. Sci., *12*, 1463–1467.

Codrington, H.W., A Short History of Ceylon (Asian Educational Services, New Delhi Madras, 1994).

Dahanayake, K. and Kulasena N. (2008a), *Geological evidence for Palaeo-Tsunami in Sri Lanka*, Sci. Tsunami Hazards., *27*, 54.

Dahanayake, K and Kulasena, N. (2008b), *Recognition of diagnostic criteria for recent- and palaeo-tsunami sediments from Sri Lanka*, Marine Geology, *254*, 180–186.

Dawson, A.G., Shi, S., Dawson, S., Takahashi, T. and Shuto, N. (1996a), *Coastal sedimentation associated with the June 2nd and 3rd, 1994 Tsunami in Rajegwesi, Java*. Quaternary Science Reviews, *15*, 901–912.

Dawson, S., Smith, D. E., Ruffman, A., and Shi, S. (1996b), *The diatom biostratigraphy of tsunami sediments: Examples from recent and middle Holocene events*, Phys. Chem. Earth, *21*, 87–92.

Duller, G. A. T., Luminescence Dating: Guidelines on using luminescence dating in archaeology (English Heritage, Swindon 2008).

Engel M. and Brückner H., (2011), *The identification of palaeotsunami deposits: a major challenge in coastal sedimentary research*, Coastline Reports *17*, 65–80.

EZZY T. R., HUFTILE G. J. and COX M. E. Applying ground penetrating radar (GPR) to improve hydrogeological understanding and groundwater modelling within a coastal plain setting, Tecnología de la intrusión de agua de mar en acuíferos costeros: países mediterráneos (IGME, Madrid 2003. ISBN 84-7840-470-8).

FINE I. V., RABINOVICH, A. B. and THOMSON, R. E. (2005), *The dual source region for the 2004 Sumatra Tsunami*, Geophys. Res. Lett., *32*, L16602, doi:10.1029/2005GL023521.

FOLK R L and WARD W C. *Brazos River bar: a study in the significance of grain size parameters*. J. Sediment. Petrol. *27*:3–26, 1957.

FUJINO, S., MASUDA, F., TAGOMORI, S., and MATSUMOTO, D., (2006*), Structure and depositional processes of a gravelly tsunami deposit in a shallow marine setting: Lower Cretaceous Miyako Group, Japan, 1*: Sedimentary Geology, *187*, 127–138.

GOTO, K., CHAGUÉ-GOFF, C., FUJINO, S., GOFF, J.R., JAFFE, B.E., NISHIMURA, Y., RICHMOND, B.M., SUGAWARA, D., SZCZUCIŃSKI, W., TAPPIN, D.R., WITTER, R.C., YULIANTO, E., (2011), *New insights of tsunami hazard from the 2011 Tohoku-oki event*, Marine Geology *290* (1–4), 46–50.

HARDY S., R., The legends and theories of the Buddhists compared with history and science: with introductory notices of the life and system of Gothama Buddha, (Williams and Norgate, 14, Henrietta street, Covent garden. London, 1866).

HASHIMOTO, T, KOYANAGI, A, YOKOSAKA, K., HAYASHI, Y and SOTOBAYASHI, T (1986), *Thermoluminescence colour images from quartz of beach sands*, Geochemical J. *20*, 111–18.

HAVHOLM, K.G., BERGSTROM, N.D., JOL, H.M. and RUNNING, G.L., GPR survey of a Holocene aeolian/fluvial/lacustrine succession, Lauder Sandhills, Manitoba, Canada. In Ground Penetrating Radar in Sediments (eds. Bristow, C.S. and Jol, H.M.). (The Geological Society, London, Special Publication, 211, 2003), pp. 47–54.

HEINZ, J. and AIGNER, T., Three-dimensional GPR analysis of various Quaternary gravel-bed braided river deposits (southwestern Germany). In Ground Penetrating Radar in Sediments (eds. Bristow, C.S. and Jol, H. M.). (Geological Society, London, Special Publications, 2003, 211), pp 99–110.

HERATH, J.W., The Economic Geology of Sri Lanka (Natural Resource Series No 1, NARESA Publication 1985).

HERATH, M. M. J. W., Sri Lankan beach mineral sands (Geological Survey Publication. Sri Lanka, 1988).

HETTIARACHCHI, S.S.L. and SAMARAWICKRAMA, S.P. (2005), Experience of the Indian Ocean Tsunami on the Sri Lankan coast. International Symposium on Disaster Reduction on Coasts, Monash University, Melbourne, Australia.

HINDSON, R.A. and ANDRADE, C. (1999), *Sedimentation and hydrodynamic processes associated with the tsunami generated by the 1755 Lisbon earthquake*, Quaternary International, *56*, 27–38.

HUNTLEY, D.J. and CLAGUE, J.J. (1996), *Optical dating of tsunami-laid sands*, Quaternary Research, *46*, 127–140.

JACKSON K.L., EBERLI, G.P., AMELUNG, F., MCFADDEN, M.A., MOORE A.L., RANKEY, E.C. and JAYASENA H. A. H., (2014), H*olocene Indian Ocean tsunami history in Sri Lanka*, Geology *42* (10), 859–862.

JAFFE, B., GELFENBAUM, G., RUBIN, D., PETERS, R., ANIMA, R., SWENSSON, M., OLCESE, D. BERNALES L., GOMEZ, J., and RIEGA, P. (2003), Tsunami Deposits: Identification and Interpretation of Tsunami Deposits from the June 23, 2001 Peru Tsunami, In Proceedings of the International Conference on Coastal Sediments 2003, CD-ROM Published by World Scientific Publishing Corp and East Meets West Productions, Corpus Christi, TX, USA. ISBN 981-238-422-7.

JAFFE, B. E. and GELFENBAUM, G. (2007), *A simple model for calculating tsunami flow speed from tsunami deposits*. Sedimentary Geology, *200*, 347–361.

JANKAEW K., ATWATER B.F., SAWAI Y., CHOOWONG M., CHAROENTITIRAT, T., MARTIN, M.E. and PRENDERGAST, A. (2008), *Medieval forewarning of the 2004 Indian Ocean tsunami in Thailand*, Nature, *455*, 1228–1231.

JOL H. M., Ground Penetrating Radar Theory and Applications (Elsevier, 2008).

JOL H. M., and BRISTOW C. S., GPR in sediments: Advice on data collection, basic processing and interpretation, a good practice guide, in Ground Penetrating Radar in Sediments (eds. Bristow C. S., and Jol H. M.,), (Geol. Soc. London, 2003), pp. 9–27.

KATO, Y., and M. KIMURA (1983), *Age and origin of so-called "Tsunami-ishi", Ishigaki island, Okinawa prefecture*, J. Geol. Soc. Japan, *89*, 471–474.

KATUPOTHA J. and FUJIWARA, K. (1988), *Holocene sea level change on the southwest and south coasts of Sri Lanka*, Palaeogeography, Palaeoclimatology, Palaeoecology, *68*, 189–203.

KORYCANSKY, D.G. and LYNETT, P.J. (2007), *Runup from impact tsunami*, Geophysical Journal International, *170*, 1076–1088.

KOSTER, B., HADLER, H., VÖTT, A. and REICHERTER, K. (2013), *Application of GPR for visualising spatial distribution and internal structures of tsunami deposits—Case studies from Spain and Greece*, Zeitschrift für Geomorphologie, Supplementary Issues, *57*(4), 29–45.

KOSTER B., HOFFMANN G., GRÜTZNER C. and REICHERTER, K. (2014), *Ground penetrating radar facies of inferred tsunami deposits on the shores of the Arabian Sea (Northern Indian Ocean)*, Marine Geology *351*(2014) 13–24.

LE ROUX, J.P. and VARGAS, G. (2005), *Hydraulic behaviour of tsunami backflows: insights from their modern and ancient deposits*, Environmental Geology, *49*, 65–75.

LE ROUX, J.P. and VARGAS, G. (2007), *Structure and depositional processes of a gravelly tsunami deposit in a shallow marine setting: Lower Cretaceous Miyako Group, Japan—discussion*, Sedimentary Geology, *201*, 485–487.

MÄTZLER C. and MURK A., Complex dielectric constant of dry sand in the 0.1 to 2 GHz range (Research Report No. 2010-06-MW, Institute of Applied Physics, University of Bern, Sidlerstrasse 5, 3012 Bern, Switzerland, 2010).

MEYERS, R. A., SMITH, D. G., JOL, H. M. and PETERSON, C. D. (1996), *Evidence for eight great earthquake-subsidence events detected with ground-penetrating radar, Willapa barrier, Washington*. Geology, *24*, 99–102.

MONECKE, K., FINGER, W., KLARER, D., KONGKO, W., MCADOO, B.G., MOORE, A.L. and SUDRAJAT, S.U. (2008), *A 1,000-year sediment record of tsunami recurrence in northern Sumatra*. Nature, *455*, 1232–1234.

MOORE, A.L. (2000), *Landward fining in onshore gravel as evidence for a late Pleistocene tsunami on Molokai, Hawaii*, Geology, *28*, 247–250.

MOORE, A.L., MCADOO, B.G., and RUFFMAN, A. (2007), *Landward fining from multiple sources in a sand sheet deposited by the 1929 Grand Banks tsunami, Newfoundland*: Sedimentary Geology, *200*, 336–346.

MORTON, R.A., GELFENBAUM, G., and JAFFE, B.E. (2007), *Physical criteria for distinguishing sandy tsunami and storm deposits using modem examples*: Sedimentary Geology, *200*, 184–207.

MORTON, R.A., GOFF, J.R., and NICHOL, S.L. (2008), *Hydrodynamic implications of textural trends in sand deposits of the 2004 tsunami in Sri Lanka*, Sedimentary Geology, *207*, 56–64.

MURRAY, A, S. and WINTLE, A G. (2000), *Luminescence dating of quartz using an improved single-aliquot regenerative-dose protocol*, Radiation Measurements *32*, 57–73.

PELINOVSKY E., CHOI B.H., STROMKOV A., DIDENKULOVA I., and KIM H.-S. (2005), Analysis of Tide-Gauge Records of the 1883 Krakatau Tsunami, In Tsunamis (ed. K.Satake), (Springer, Netherlands), pp. 57–78.

PETERS, R., JAFFE, B., and GELFENBAUM, G. (2007), *Distribution and sedimentary characteristics of tsunami deposits along the Cascadia margin of western North America*, Sedimentary Geology, *200*, 372–386.

PRATT, B.R. AND BORDONARO, O.L. (2007), *Tsunamis in a stormy sea: Middle Cambrian inner-shelf limestones of Western Argentina*, Journal of Sedimentary Research, *77*, 256–262.

PREMASIRI H. M. R., Identification of palaeotsunami deposits using ground penetrating radar, sedimentological and micropaleontological techniques; implications for Sri Lankan tsunami hazard (Ph.D. Thesis, Keele University, Staffordshire, UK, 2012) 284 pp.

PRENDERGAST A. L., CUPPER, M. L., JANKAEW K. and SAWAI, Y. (2012), *Indian Ocean tsunami recurrence from optical dating of tsunami sand sheets in Thailand*, Marine Geology, 295–298.

RANASINGHAGE, P.N., Holocene coastal development in southeastern-eastern Sri Lanka: Paleodepositional environments and paleo-coastal hazards (Ph.D. thesis, Kent State University, Kent, Ohio, 2010, 437 pp.).

RUIZ, F., ABAD, M., VIDAL, J.R., CACERES, L.M., GONZALEZ-REGALADO, M.L., CARRETERO, M.I., POZO, M., and TOSCANO, F.G. (2008), *The geological record of the oldest historical tsunamis in southwestern Spain*, Rivista Italiana di Paleontologia e Stratigrafia, *114*, 145–154.

SMITH, D.E., SHI, S., CULLINGFORD, R.A., DAWSON, A.G., DAWSON, S., FIRTH, C.R., FOSTER, I.D.L., FRETWELL, P.T., HAGGART, B.A., HOLLOWAY, L.K., and LONG, D. (2004), *The Holocene Storegga slide Tsunami in the United Kingdom*, Quaternary Science Reviews, *23*, 2291–2321.

SOULSBY, R., SMITH, D., and RUFFMAN, A., Reconstructing Tsunami Runup from Sedimentary Characteristics—A Simple Mathematical Model, In Coastal Sediments (eds. Kraus, N.C. and Rosati, J.D.) (American Society of Civil Engineers, 2007), pp.1075-1088.

SPISKE, M., PIEPENBREIER, J., BENAVENTE, C. and BAHLBURG, H. (2013), *Preservation potential of tsunami deposits on arid siliciclastic coasts*, Earth-Science Reviews *11*, 126, 58–73.

STYLES, P., SHRIRA, V. and PREMASIRI H. M. R. (2007), *Sumatra tsunami signature in sediment characteristics on the Sri Lankan coast*, Geophysical Research Abstracts, Vol. *9*, 05310, SRef-ID: 1607-7962/gra/EGU2007-A-05310.

STYLES, P., Environmental Geophysics, (ISBN: 978-90-73834-33-0, EAGE Publications bv., 2011).

SUMANGALA, H, The Mahawamsa, first thirty-six chapters (Godage Brothers Colombo 1996),

SURAWEERA, A. V., A comprehensive account of the Kings of Sri Lanka (Rathmalana, Colombo 2000).

SWITZER, A.D., BRISTOW, C.S., and JONES, B.G. (2006), *Investigation of large-scale washover of a small barrier system on the southeast Australian coast using ground penetrating radar*. Sedimentary Geology, *183*, 145–156.

SYVITSKI, J. P. M., (ed)., Principles, Methods and Application of Particle Size Analysis (Cambridge University Press 1991).

TAMURA, T., MURAKAMI, F., NANAYAMA, F., WATANABE, K., SAITO, Y. (2008), *Ground-penetrating radar profiles of Holocene raised-beach deposits in the Kujukuri strand plain, Pacific coast of eastern Japan*, Marine Geology, *248*, 11–27.

WAGNER, J. F. and CHANCHAI, S. (2011), Grain-Size and Thin Section Characteristics of Tsunami Sediments from Thai-Andaman Coast, Thailand. In The Tsunami Threat—Research and Technology (ed. Nils-Axel Marner, ISBN: 978-953-307-552-5). http://cdn.intechopen.com/pdfs-wm/13086.pdf.

WAGNER J.-F. and SRISUTAM C. (2011), Grain-Size and Thin Section Characteristics of Tsunami Sediments from Thai-Andaman Coast, Thailand. The Tsunami Threat—Research and Technology, Nils-Axel Marner (Ed.), ISBN: 978-953-307-552-5, InTech. Available from: http://www.intechopen.com/books/thetsunami-threat-research-and-technology/grain-size-and-thin-section-characteristics-of-tsunami-sedimentsfrom-thai-andaman-coast-thailand.

WALLINGA, J. (2002), *Optically stimulated luminescence dating of fluvial deposits: a review*. Boreas *31*, 303–322.

WATTEGAMA, C., (2005), The Seven Tsunamis That Hit The Isle of Lanka, WWW Virtual Library—Sri Lanka, http://www.lankalibrary.com/news/tsunamis2.htm.

WEISS, R., (2008), *Sediment grains moved by passing tsunami waves: Tsunami deposits in deep water*, Marine Geology, *250*, 251–257.

WIJETUNGA W. M., (2008), The Present Status of the Home gardens in Galle District of Sri Lanka Affected by the December 26, 2004 Tsunami: A Comparison with Non-affected Home gardens in Connection with Restoration, Unpublished PhD Thesis, University of Natural Resources and Applied Life Sciences (BOKU), Vienna.

WITTER, R.C., KELSEY, H.M. and HEMPHILL-HALEY, E. (2001), *Pacific storms, El Nino and tsunamis: Competing mechanisms for sand deposition in a coastal marsh, Euchre Creek, Oregon*, Journal of Coastal Research, *17*, 563–583.

WOODROFFE, S.A. and HORTON, B.P. (2005), *Holocene sea-level changes in the Indo-Pacific*, Journal of Asian Earth Sciences, *25*, 29–43.

WOODWARD, J., ASHWORTH, P.J., BEST, J.L., SAMBROOK SMITH, G.H. and SIMPSON, C.J., The use and application of GPR in sandy fluvial environments: methodological considerations, In Ground penetrating radar in sediments.(eds. C.S. Bristow and H.M. Jol) (Geological Society, London, Special Publications 211, 2003), pp. 127–142.

YAN, Z. and TANG, D. (2008), *Changes in Suspended Sediments Associated with 2004 Indian Ocean Tsunami*, Advances in Space Research *43*, 89–95.

(Received October 29, 2014, revised June 17, 2015, accepted June 18, 2015, Published online July 8, 2015)